

# NNLO QCD corrections to the resonant sneutrino/slepton production at Hadron Colliders

Swapan Majhi\* and Prakash Mathews†

Saha Institute of Nuclear Physics, 1/AF Bidhannagar,  
Kolkata 700064, India.

V Ravindran‡

Regional Centre for Accelerator based Particle Physics,  
Harish-Chandra Research Institute, Chhatnag Road, Jhusi,  
Allahabad 211 019, India.

## Abstract

We present a complete next to next to leading order QCD corrections to the resonant sneutrino and charged slepton production cross sections at hadronic colliders such as the Tevatron and the Large Hadron Collider within the context of  $R$ -parity violating supersymmetric model. We have demonstrated the role of these corrections in reducing uncertainties resulting from renormalisation and factorisation scales and thereby making our predictions reliable. We have incorporated soft gluon effects at  $N^3LO$  level in order to study the stability of our results under perturbation. The NNLO corrections are found to be large and significant. The results obtained in this article are also applicable to resonance production of any color-neutral scalar.

---

\*swapan.majhi@saha.ac.in

†prakash.mathews@saha.ac.in

‡ravindra@hri.res.in

# 1 Introduction

The Standard Model (SM) of particle physics is undoubtedly a very successful model even though its scalar sector remains in an unsatisfactory state of affairs. This is because of the fact that the Higgs boson in the scalar sector which is responsible for symmetry breaking mechanism is still missing. There are also other issues such as gauge hierarchy problem, dark matter, baryogenesis, gauge unification etc., that are still not fully understood within the framework of the SM, pointing to physics beyond the standard model. In the past, the above mentioned issues were being addressed by going beyond the SM. Two of the most attractive classes of such models contain features incorporating supersymmetry [1] and/or grand unification [2] (scenarios with a low intermediate scale [3]). These models contain large number of new particles including new scalars. The couplings of the first generation SM fermions to these new scalars need not be suppressed. This provides us a new platform to study their potential new physics signals.

The electroweak gauge invariance ensures both baryon ( $B$ ) and lepton ( $L$ ) number conservations within the SM, but this is not the case for supersymmetry (SUSY). The most general superpotential respecting the gauge symmetry of the SM contains bilinear and trilinear terms which do not respect  $B$  or  $L$  conservations. A discrete symmetry called  $R$ -parity can be used to forbid such terms. The corresponding conserved quantum number is given by  $R_p \equiv (-1)^{3B+L+2S}$ , where  $S$  is the spin of the particle. In the minimal supersymmetric standard model (MSSM), this symmetry has been originally imposed to suppress the rapid proton decay, it also guarantees stability of lightest supersymmetric particle (LSP) and hence a natural candidate for cold dark matter.

The introduction of this symmetry is *not* the only option to suppress proton decay, there exists several alternatives through introduction of other symmetries. Hence, it is of phenomenological interest to consider possible violations of  $R$ -parity and study their experimental consequences.

The possible  $R$ -parity violating ( $\mathcal{R}_p$ ) terms in the superpotential can be parametrised as

$$\mathcal{W}_{\mathcal{R}_p} = \mu_i L_i H_2 + \lambda_{ijk} L_i L_j E_k^c + \lambda'_{ijk} L_i Q_j D_k^c + \lambda''_{ijk} U_i^c D_j^c D_k^c, \quad (1)$$

where  $L_i$  and  $Q_i$  are the  $SU(2)$ -doublet lepton and quark superfields,  $E_i^c, U_i^c, D_i^c$  the singlet superfields and  $H_i$  the Higgs superfields. Note that  $\lambda_{ijk}$  is antisymmetric under the interchange of the first two indices and  $\lambda''_{ijk}$  is antisymmetric under the interchange of the last two. The first three terms in eqn.(1) violate  $L$  and the last term violates  $B$  conservation. We need to have at least one of the two sets of couplings to be vanishingly small in order to satisfy the constraints coming from the non-observance of proton decay. In the following, we assume that  $B$  is a good symmetry of the theory, or in other words all of  $\lambda''_{ijk}$  are zero. This can also suppress all dimension six operators leading to proton decay (see [4]) along with the dimension five ones. In [4, 5], this scenario has been motivated within certain theoretical frameworks and makes simpler, problem of preservation of GUT-scale baryon asymmetry [6]. The presence of the other  $\mathcal{R}_p$  terms can affect the baryon asymmetry of the universe. Fortunately these bounds are highly model-dependent and hence we evade them (see [7]).

Each interaction in eqn.(1) has its unique experimental signatures through low-energy phenomenology and/or in resonance production at colliders. Large number of bounds on these coupling result from the studies of low and intermediate energy processes, namely rare decays with lepton and/or hadron flavor violation. The neutral and charged current universality in lepton and quark sectors, high precision measurements in anomalous magnetic and electric dipole moments and observables with CP violation provide stringent constraints on these couplings at low energies. Terms involving  $\lambda_{ijk}$  lead to resonant sneutrino production in  $e^+e^-$  collider [8, 9] and those involving  $\lambda''_{ijk}$  lead to resonant squark production in hadron-hadron collisions [10, 11]. Similarly, the  $\lambda'_{ijk}$  terms can contribute to both resonant squark production at an  $e^\pm p$  colliders [12] as well as to resonant charged slepton and sneutrino production at hadron colliders [10, 13]. A simplified search strategy at colliders could be to assume the existence of one dominant R-parity violating coupling at a time. In the past most of the studies rely on this assumption. Since the absence of tree-level flavor changing neutral current processes lead to severe constraints on the simultaneous presence of more than one  $\lambda'_{ijk}$  [14], we shall restrict ourselves to only one non-zero  $\lambda'_{ijk}$ . In the rest of the paper, we will concentrate only on the  $\lambda'_{ijk}$  couplings that can affect the resonant production. That part of the Lagrangian can be written in terms of the component fields as

$$\begin{aligned} \mathcal{L}_{\lambda'} = & \lambda'_{ijk} \left[ \overline{d_{kR}} \nu_{iL} \tilde{d}_{jL} + \overline{d_{kR}} d_{jL} \tilde{\nu}_{iL} + \overline{(\nu_{iL})^c} d_{jL} \tilde{d}_{kR}^* \right. \\ & \left. - \overline{d_{kR}} \ell_{iL} \tilde{u}_{jL} - \overline{d_{kR}} u_{jL} \tilde{\ell}_{iL} - \overline{(\ell_{iL})^c} u_{jL} \tilde{d}_{kR}^* \right] + \text{h.c.} \end{aligned} \quad (2)$$

The squarks in supersymmetric theories behave as leptoquarks and the charged sleptons/sneutrinos behave as charged/neutral Higgses of multi-Higgs-doublet scenario. Hence, one would expect non-zero values for these couplings will have important phenomenological consequences.

Quantum Chromodynamics (QCD) plays an important role in hadron colliders as the underlying scattering processes involve quarks (anti-quarks) and gluons. The leading order (LO) scattering processes involving quarks (anti-quarks) and gluons often predict results that are sensitive to large theoretical uncertainties through non-perturbative parton densities and missing higher order perturbative radiative corrections. In the next sections, we will elaborate on the sources of these uncertainties and provide systematic methods to reduce them. In [15], first results on the next-to-leading order (NLO) QCD corrections to sneutrino and charged slepton productions at hadron colliders were reported. These results were later confirmed and further NLO SUSY-QCD corrections were systematically incorporated in the analysis by the authors of [16]. It was found that the NLO QCD effects were quite large  $\sim 10\% - 40\%$  at both Tevatron as well as LHC and hence they were used by both CDF [17] and D0 [18] collaboration to analyse their data (Run-I as well as Run-II data). In their analysis to set bound on these R-parity violating couplings, K-factor for SM background [] was considered at the next to next to leading order (NNLO) level while for the R-parity violating effects only NLO K-factor was used. Therefore, it is desirable to compute the K-factors for the resonant sneutrino and/or charged slepton productions at NNLO in QCD. These results will quantitatively improve the analysis based on high statistics data available in the ongoing and future experiments. From the theoretical point of view, higher order radiative corrections provide

a test of the convergence of the perturbation theory and hence the reliable comparison of data with the theory predictions is possible. We have also studied the effects of soft gluons which often dominate at hadronic collisions. This also opens up the possibility of resumming them to all orders in perturbation theory through suitable framework. The fixed order perturbative results most often suffer from large uncertainties due to the presence of renormalisation and factorisation scales. They get reduced as we include more and more terms in the perturbative expansion thanks to renormalisation group invariance. It is also important to estimate the uncertainties coming from the choice of parton density sets available in the literature. Due to these reasons, we think that it is worthwhile to perform the next-next-to-leading order (NNLO) calculation to the aforementioned processes. In our previous paper [15], we used fixed  $\mathcal{R}_p$  coupling ( $\lambda' = 0.01$ ) based on the assumption that its scale dependence is very weak, in addition the *value* of the coupling  $\lambda'$  was immaterial and only served to set an overall normalisation for the cross-section. In the present paper we have systematically included its scale dependence through the renormalisation group equations and we will discuss the impact of it in the next sections.

We briefly review the constraints on  $\lambda'$  from low-energy phenomenology. Non-zero  $\lambda'$ s can lead to additional four-fermion operators that may contribute to meson decays, neutral meson mixing, some of which may be forbidden otherwise. In Table 1, we list the currently known bounds on several of these couplings<sup>1</sup>. The strongest bound is on  $\lambda'_{111}$  and is derived from non-observation of neutrinoless double beta decay (*a*) [20]. The others are much weaker and are derived from (*b*) upper bound on the mass of the  $\nu_e$  [5, 21–23]; data on (*c*) charged-current universality [9]; (*d*) atomic parity violation [24]; (*e*)  $\tau \rightarrow \pi\nu_\tau$  and  $D \rightarrow Kl\nu$  [22]; and (*f*)  $D^0$ - $\bar{D}^0$  mixing [14]. Since these bounds are derived from effective

$\{ijk\}$	Existing bounds	$\{ijk\}$	Existing bounds	$\{ijk\}$	Existing bounds
111	0.001 <sup>a)</sup>	211	0.09 <sup>e)</sup>	311	0.10 <sup>e)</sup>
112	0.02 <sup>c)</sup>	212	0.09 <sup>e)</sup>	312	0.10 <sup>e)</sup>
121	0.035 <sup>d)</sup>	221	0.18 <sup>e)</sup>	321	0.20 <sup>f)</sup>
122	0.02 <sup>b)</sup>	222	0.18 <sup>e)</sup>	322	0.20 <sup>f)</sup>

Table 1: The upper bounds on the  $\lambda'$ -type  $\mathcal{R}_p$  couplings of interest for a common sfermion mass  $\tilde{m} = 100$  GeV. The superscripts refer to the specific experiments leading to the constraints and as described in the text.

four-fermion operators, they typically scale like the mass of the exchanged sfermion<sup>2</sup>. These bounds are actually applicable only to particular combinations of couplings and masses and reduce to those in the table only under the assumption of only one coupling being non-zero. In addition, in meson decays, most often it is the squark that is exchanged; hence charged sleptons/sneutrinos could very well be much lighter without contradicting the bounds.

<sup>1</sup>A more complete list can be found in refs. [19].

<sup>2</sup>Of those listed in Table 1, the only exceptions to this rule are the bounds for  $\lambda'_{111}$  and  $\lambda'_{122}$  [5, 20–22].

In the next section, we describe the computation of resonant production of scalar/pseudo scalar to NNLO in perturbative QCD. The results are obtained in the  $\overline{MS}$  scheme. We then proceed to study the impact of our results on their production cross sections for both Tevatron and LHC energies. Finally we summarise our findings in the conclusion. Our analytical results that go into the numerical code are presented in the Appendix.

## 2 Computation of partonic coefficient functions to order $\alpha_s^2$

In this section, we describe in detail, the computation of second order ( $\alpha_s^2$ ) QCD radiative corrections to resonant production, in hadron colliders, of a neutral scalar particle  $\phi(\xi)$  which couple to fermionic fields  $\psi(\xi)$  through Yukawa interaction given by the action:

$$S = \int d^4\xi \mathcal{L}_{int}(\xi) = \lambda' \int d^4\xi \phi(\xi) \bar{\psi}(\xi)\psi(\xi) \quad (3)$$

where  $\lambda'$  is the coupling strength of the interaction. We present our results in such a way that they can be used for a similar study on charged scalar production as well and hence are applicable to a detailed study on resonant production of sneutrinos and charged sleptons which is the main goal of this present work. The inclusive hadronic cross section for the reaction

$$H_1(P_1) + H_2(P_2) \rightarrow \phi(p_5) + X, \quad (4)$$

is given by

$$\sigma_{\text{tot}}^{\phi} = \frac{\pi\lambda'^2(\mu_R^2)}{12S} \sum_{a,b=q,\bar{q},g} \int_{\tau}^1 \frac{dx_1}{x_1} \int_{\tau/x_1}^1 \frac{dx_2}{x_2} f_a(x_1, \mu_F^2) f_b(x_2, \mu_F^2) \Delta_{ab} \left( \frac{\tau}{x_1 x_2}, m_{\phi}^2, \mu_F^2, \mu_R^2 \right)$$

with  $\tau = \frac{m_{\phi}^2}{S}$  ,  $S = (P_1 + P_2)^2$  ,  $p_5^2 = m_{\phi}^2$ , (5)

where  $H_1$  and  $H_2$  denote the incoming hadrons and  $X$  represents an inclusive hadronic state. The parton densities denoted by  $f_c(x_i, \mu_F^2)$  ( $c = q, \bar{q}, g$ ) depend on the scaling variables  $x_i$  ( $i = 1, 2$ ) through  $p_i = x_i P_i$  and the mass factorization scale  $\mu_F$ . Here  $p_i$  ( $i = 1, 2$ ) are the momenta of incoming partons namely quarks, anti-quarks and gluons. The coupling constant  $\lambda'$  gets renormalised at the renormalisation scale  $\mu_R$  due to ultraviolet singularities present in the theory. The factorisation scale is introduced on the right hand side of the above equation to separate long distant dynamics from the perturbatively calculable short distant partonic coefficient functions  $\Delta_{ab}$ .  $\Delta_{ab}$  depends on both  $\mu_R$  and  $\mu_F$  in such a way that the entire scale dependence goes away to all orders in perturbation theory when convoluted with appropriate parton densities. This is due to the fact that the observable on the left hand side of the above equation is renormalisation group (RG) invariant with respect to both the scales. This implies

$$\mu^2 \frac{d\sigma_{\text{tot}}^{\phi}}{d\mu^2} = 0, \quad \mu = \mu_F, \mu_R, \quad (6)$$

$$\mu_R^2 \frac{d}{d\mu_R^2} \left[ \lambda'^2(\mu_R^2) \Delta_{ab}(x, m_\phi^2, \mu_F^2, \mu_R^2) \right] = 0. \quad (7)$$

The partonic coefficient functions that appear in eqn.(5) are computable in perturbative QCD in terms of strong coupling constant  $g_s$ . The ultraviolet singularities present in the theory are regularised in dimensional regularisation and are removed in  $\overline{MS}$  scheme, introducing the renormalisation scale  $\mu_R$  at every order in perturbative expansion. In addition, the Yukawa coupling  $\lambda'$  also gets renormalised due to strong interaction dynamics. Hence, for our computation, we require only two renormalisation constants to obtain UV finite partonic coefficient functions,  $\Delta_{ab}$ . These constants are denoted by  $Z(\mu_R)$  and  $Z_{\lambda'}(\mu_R)$ , where the former renormalises the strong coupling constant  $g_s$  and the later Yukawa coupling  $\lambda'$ .

We define the bare strong coupling constant by  $\hat{a}_s = \hat{g}_s^2/16\pi^2$ ,  $\hat{g}_s$  being the dimensionless strong coupling constant in  $n = 4 + \epsilon$ , with  $n$  being the number of space time dimensions. The bare coupling constant  $\hat{a}_s$  is related to the renormalised one,  $a_s(\mu_R^2)$  by the following relation:

$$S_\epsilon \hat{a}_s = Z(\hat{a}_s, \mu^2, \mu_R^2, \epsilon) a_s(\mu_R^2) \left( \frac{\mu^2}{\mu_R^2} \right)^{\frac{\epsilon}{2}}. \quad (8)$$

The scale  $\mu$  comes from the dimensional regularisation in order to make the bare coupling constant  $\hat{g}_s$  dimensionless in  $n$  dimensions.  $S_\epsilon$  is the spherical factor characteristic of  $n$ -dimensional regularisation.

The renormalisation constant that relates the bare coupling constant  $\hat{a}_s$  to the renormalised one  $a_s(\mu_R^2)$  through the eqn.(8) is given by

$$\begin{aligned} Z(\hat{a}_s, \mu^2, \mu_R^2, \epsilon) = 1 &+ \hat{a}_s \left( \frac{\mu_R^2}{\mu^2} \right)^{\frac{1}{2}\epsilon} S_\epsilon \left[ \frac{2\beta_0}{\epsilon} \right] + \hat{a}_s^2 \left( \frac{\mu_R^2}{\mu^2} \right)^\epsilon S_\epsilon^2 \left[ \frac{\beta_1}{\epsilon} \right] \\ &+ \hat{a}_s^3 \left( \frac{\mu_R^2}{\mu^2} \right)^{\frac{3}{2}\epsilon} S_\epsilon^3 \left[ -\frac{4\beta_0 \beta_1}{3\epsilon^2} + \frac{2\beta_2}{3\epsilon} \right] + \mathcal{O}(\hat{a}_s^4). \end{aligned} \quad (9)$$

The coefficients  $\beta_i$  for  $i = 1, \dots, 4$  can be found in [25] for  $SU(N)$  QCD expressed in terms of the color factors:

$$C_A = N, \quad C_F = \frac{N^2 - 1}{2N}, \quad T_F = \frac{1}{2}. \quad (10)$$

and  $n_f$  is the number of active flavors. Similarly, for the Yukawa coupling, we have

$$S_\epsilon \hat{\lambda}' = Z_{\lambda'}(\hat{a}_s, \mu^2, \mu_R^2, \epsilon) \lambda'(\mu_R^2) \left( \frac{\mu^2}{\mu_R^2} \right)^{\frac{\epsilon}{2}}, \quad (11)$$

where

$$Z_{\lambda'}(\hat{a}_s, \mu^2, \mu_R^2, \epsilon) = 1 + \hat{a}_s \left( \frac{\mu_R^2}{\mu^2} \right)^{\frac{\epsilon}{2}} S_\epsilon \left[ \frac{1}{\epsilon} \left( 2 \gamma_0 \right) \right] + \hat{a}_s^2 \left( \frac{\mu_R^2}{\mu^2} \right)^\epsilon S_\epsilon^2 \left[ \frac{1}{\epsilon^2} \left( 2 \left( \gamma_0 \right)^2 - 2 \beta_0 \gamma_0 \right) \right]$$

$$\begin{aligned}
& + \frac{1}{\epsilon} \left( \gamma_1 \right) \Big] + \hat{a}_s^3 \left( \frac{\mu_R^2}{\mu^2} \right)^{3\frac{\epsilon}{2}} S_\epsilon^3 \left[ \frac{1}{\epsilon^3} \left( \frac{4}{3} (\gamma_0)^3 - 4 \beta_0 (\gamma_0)^2 + \frac{8}{3} \beta_0^2 \gamma_0 \right) \right. \\
& \left. + \frac{1}{\epsilon^2} \left( 2 \gamma_0 \gamma_1 - \frac{2}{3} \beta_1 \gamma_0 - \frac{8}{3} \beta_0 \gamma_1 \right) + \frac{1}{\epsilon} \left( \frac{2}{3} \gamma_2 \right) \right] + \mathcal{O}(\hat{a}_s^4). \quad (12)
\end{aligned}$$

The anomalous dimensions  $\gamma_i$  for  $i = 1, \dots, 4$  can be obtained from the quark mass anomalous dimensions given in [26]. While the  $\mathcal{O}(\hat{a}_s^3)$  terms in both  $Z$  and  $Z_{\lambda'}$  do not contribute to partonic sub processes computed to order  $a_s^2$ , they determine the scale evolution of both  $a_s$  and  $\lambda'$  to NNLO through renormalisation group equations:

$$\begin{aligned}
\mu_R^2 \frac{d}{d\mu_R^2} \ln a_s(\mu_R^2) &= - \sum_{i=1}^{\infty} a_s^i(\mu_R^2) \beta_{i-1}, \\
\mu_R^2 \frac{d}{d\mu_R^2} \ln \lambda'(\mu_R^2) &= - \sum_{i=1}^{\infty} a_s^i(\mu_R^2) \gamma_{i-1}. \quad (13)
\end{aligned}$$

and constitute dominant soft gluon contribution to order  $\alpha_s^3$ . The perturbatively calculable  $\Delta_{ab}$  can be expanded in powers of strong coupling constant  $a_s(\mu_R^2)$  as

$$\Delta_{ab} \left( x, m_\phi^2, \mu_F^2, \mu_R^2 \right) = \sum_{i=0}^{\infty} a_s^i(\mu_R^2) \Delta_{ab}^{(i)} \left( x, m_\phi^2, \mu_F^2, \mu_R^2 \right)$$

$\Delta_{ab}$  gets contributions from various partonic reactions.

Having studied the UV renormalisation constants relevant for our computation, we now list out various partonic sub processes that will contribute to NNLO order ( $\alpha_s^2$ ). The leading order partonic reaction (fig.(1)) is given by

$$q_i + \bar{q}_j \rightarrow \phi \quad (14)$$

and its contribution is found to be proportional to  $\delta(1-x)$  where  $x = m_\phi^2/s$  with partonic center of mass energy  $s = (p_1 + p_2)^2$ . At NLO (fig.(2,3,4)), we have

$$\begin{aligned}
q_i + \bar{q}_j &\rightarrow \phi + \text{one loop}, \\
q_i + \bar{q}_j &\rightarrow \phi + g, \\
q_i(\bar{q}_i) + g &\rightarrow \phi + q_j(\bar{q}_j). \quad (15)
\end{aligned}$$

The subscripts  $i, j$  in the quark (anti-quark) fields denote the flavor indices. If  $i = j$ , then  $\phi$  will be neutral scalar otherwise it will denote a charged scalar.

At NNLO, there are several new channels open up and we discuss them one by one:

- processes with quark anti-quark pair in the initial state with no gluon (fig.(5)), one gluon (fig.(6)) and two gluons (fig.(7)) in the final state along with  $\phi$ :

$$\begin{aligned}
q_i + \bar{q}_j &\rightarrow \phi + \text{two loop}, \\
q_i + \bar{q}_j &\rightarrow \phi + g + \text{one loop}, \\
q_i + \bar{q}_j &\rightarrow \phi + g + g. \quad (16)
\end{aligned}$$

- processes (fig.(8)) with quark anti-quark pair in the final states along with  $\phi$ :

$$q_i + \bar{q}_j \rightarrow \phi + q_k + \bar{q}_l, \quad (17)$$

and quark (anti-quark) quark (anti-quark) pair in the final state with  $\phi$  (fig.(9)):

$$\begin{aligned} q_i + q_j &\rightarrow \phi + q_k + q_l, \\ \bar{q}_i + \bar{q}_j &\rightarrow \phi + \bar{q}_k + \bar{q}_l. \end{aligned} \quad (18)$$

The contributions coming from the last two reactions (eqn.(18)) will have two possibilities: the final states with identical quarks (anti-quarks) or non-identical quarks (anti-quarks). For identical quarks (anti-quarks) in the final state (fig.(10)), the number of  $t$  channel processes doubles as we need to include processes with final state quarks (anti-quarks) interchanged. We also need to appropriately multiply the statistical factor  $1/2$ .

- processes with quark (anti-quark) and gluon in the initial states

$$\begin{aligned} q_i(\bar{q}_i) + g &\rightarrow \phi + q_j(\bar{q}_j) + \text{one loop}, \\ q_i(\bar{q}_i) + g &\rightarrow \phi + q_j(\bar{q}_j) + g. \end{aligned} \quad (19)$$

- processes with pair of gluons in the initial state

$$g + g \rightarrow \phi + q_i + \bar{q}_j. \quad (20)$$

The calculation of various contributions from the partonic reactions involves careful handling of divergences that result from one [27] and two loop [28] integrations in the virtual processes and two and three body phase space integrations in the real emission processes. The loop integrals often give ultraviolet, soft and collinear divergences. But the phase space integrals give only soft and collinear singularities. Soft divergences arise when the momenta of the gluons become zero while the collinear diverges arise due to the presence of massless partons. We have regulated all the integrals in dimensional regularisation with space time dimension  $n = 4 + \epsilon$ . The singularities manifest themselves as poles in  $\epsilon$ .

We have reduced all the one loop tensorial integrals to scalar integrals using the method of Passarino-Veltman [29] in  $4 + \epsilon$  dimensions and evaluated resultant scalar integrals exactly. The form factor that contributes to reactions in eqn (16) is obtained using the dispersion technique [30] and is presented in the appendix. Two and three body phase space integrals are done by choosing appropriate Lorentz frames [31]. Since we integrate over the total phase space the integrals are Lorentz invariant and therefore frame independent. Several routines are made using the algebraic manipulation program FORM [32] in order to perform tensorial reduction of one loop integrals and two and three body phase space integrals.

The UV singularities go away after performing renormalisation through the constants  $Z$  and  $Z_{\lambda'}$ . The soft singularities cancel among virtual and real emission processes [33] at



every order in perturbation theory. The remaining collinear singularities are renormalised systematically using mass factorisation [34] as follows. For more details on the computation of NNLO QCD corrections to process of the kind considered here can be found in [35]. Let us denote the resulting UV and soft finite partonic cross sections as

$$\hat{\Delta}_{ab}(x, m_\phi^2, \mu_R^2) = \frac{S}{\lambda'^2(\mu_R^2)} \hat{\sigma}_{ab,\phi}(x, m_\phi^2, \mu_R^2),$$

where

$$\begin{aligned} \hat{\sigma}_{ab,\phi}(x, m_\phi^2, \mu_R^2) &= K_{ab} \frac{\pi}{s} Z_{\lambda'}^2 \int d^n p_5 \delta^+(p_5^2 - m^2) \sum_{m=3}^{\infty} \prod_{i=3, i \neq 5}^m \int \frac{d^n p_i}{(2\pi)^{n-1}} \delta^+(p_i^2) \\ &\quad \times \delta^{(n)}\left(\sum_{j=1}^m p_j\right) |M_{ab \rightarrow X \phi}|^2, \end{aligned}$$

$$M_{ab \rightarrow X \phi} = \langle p_1, p_2 | \hat{O}(0) | X, p_5 \rangle \quad \text{with} \quad |X, p_5\rangle = |p_3, p_4, p_6 \cdots p_m, p_5\rangle, \quad (21)$$

$\hat{O}(0)$  is the interaction operator responsible for the reactions with scalars and  $K_{ab}$  represents the spin and colour average over the initial states. Mass factorisation allows us to express the collinear singular partonic cross section  $\hat{\Delta}_{ab}$  in terms of pair of singular transition functions  $\Gamma_{cd}(x, \mu_F^2, \epsilon)$ , namely Altarelli-Parisi kernels and finite partonic coefficient function  $\Delta_{ab}$ :

$$\begin{aligned} \hat{\Delta}_{ab}(x, m_\phi^2, \mu_R^2) &= \sum_{c,d=q,\bar{q},g} \int_x^1 \frac{dx_1}{x_1} \int_{x/x_1}^1 \frac{dx_2}{x_2} \Gamma_{ca}(x_1, \mu_F^2, \epsilon) \Gamma_{db}(x_2, \mu_F^2, \epsilon) \\ &\quad \times \Delta_{cd}\left(\frac{x}{x_1 x_2}, m_\phi^2, \mu_F^2, \mu_R^2\right). \end{aligned} \quad (22)$$

The transition functions are perturbatively calculable in powers of  $a_s(\mu_F^2)$ :

$$\Gamma_{ab}(x, \mu_F^2, \epsilon) = \sum_{i=0}^{\infty} a_s^i(\mu_F^2) \Gamma_{ab}^{(i)}(x, \epsilon). \quad (23)$$

In  $\overline{MS}$  mass factorisation scheme, they are found to be (suppressing the arguments  $x$  and  $\epsilon$ )

$$\Gamma_{ab}^{(0)} = \delta_{ab} \delta(1-x), \quad (24)$$

$$\Gamma_{ab}^{(1)} = -\frac{1}{\epsilon} P_{ab}^{(0)}, \quad (25)$$

and

$$\Gamma_{ab}^{(2)} = \frac{1}{2\epsilon^2} \sum_c \left( P_{ac}^{(0)} \otimes P_{cb}^{(0)} + 2\beta_0 P_{ab}^{(0)} \right) + \frac{1}{2\epsilon} P_{ab}^{(1)}. \quad (26)$$

More explicitly we have:

$$\begin{aligned}
\Gamma_{qq}^{(2),NS} &= \Gamma_{\bar{q}\bar{q}}^{(2),NS} = \left[ \frac{1}{2\epsilon^2} \left( P_{qq}^{(0)} \otimes P_{qq}^{(0)} + 2\beta_0 P_{qq}^{(0)}(x) \right) + \frac{1}{2\epsilon} P_{qq}^{(1),NS} \right] \\
\Gamma_{\bar{q}\bar{q}}^{(2),NS} &= \Gamma_{\bar{q}\bar{q}}^{(2),NS} = \frac{1}{2\epsilon} P_{qq}^{(1),-} \\
\Gamma_{qq}^{(2),S/-} &= \Gamma_{\bar{q}\bar{q}}^{(2),S/-} = \Gamma_{\bar{q}\bar{q}}^{(2),S/-} = \Gamma_{\bar{q}\bar{q}}^{(2),S/-} = \left[ \frac{1}{2\epsilon^2} P_{gg}^{(0)} \otimes P_{gg}^{(0)} + \frac{1}{2\epsilon} P_{qq}^{(1),S/-} \right] \\
\Gamma_{gg}^{(2)} &= \Gamma_{\bar{q}\bar{q}}^{(2)} = \left[ \frac{1}{2\epsilon^2} \left\{ P_{qq}^{(0)} \otimes P_{qq}^{(0)} + P_{qq}^{(0)} \otimes P_{gg}^{(0)} + 2\beta_0 P_{qq}^{(0)} \right\} + \frac{1}{2\epsilon} P_{qq}^{(1)} \right] \quad (27)
\end{aligned}$$

In order to determine  $\Delta_{ab}$ , we set  $\mu_R = \mu_F$  and expand  $\Delta_{ab}$  (similarly  $\hat{\Delta}_{ab}$ ) as

$$\Delta_{ab} \left( x, \frac{m_\phi^2}{\mu_F^2} \right) = \sum_{i=0}^{\infty} a_s^i(\mu_F^2) \Delta_{ab}^{(i)} \left( x, \frac{m_\phi^2}{\mu_F^2} \right). \quad (28)$$

Substituting the above equation (eqn. (28)) in the eqn.(22), we obtain to order  $a_s(\mu_F^2)$

$$\begin{aligned}
\Delta_{\bar{q}\bar{q}}^{(1)} &= \hat{\Delta}_{\bar{q}\bar{q}}^{(1)} - \frac{2}{\epsilon} P_{qq}^{(0)} \otimes \hat{\Delta}_{\bar{q}\bar{q}}^{(0)} \\
\Delta_{gg}^{(1)} &= \hat{\Delta}_{gg}^{(1)} - \frac{1}{\epsilon} P_{qq}^{(0)} \otimes \hat{\Delta}_{\bar{q}\bar{q}}^{(0)} \quad (29)
\end{aligned}$$

and to order  $a_s^2(\mu_R^2)$

$$\begin{aligned}
\Delta_{\bar{q}\bar{q}}^{(2)} &= \hat{\Delta}_{\bar{q}\bar{q}}^{(2)} - 2\Gamma_{\bar{q}\bar{q}}^{(1)} \otimes \hat{\Delta}_{\bar{q}\bar{q}}^{(0)} - \frac{2}{\epsilon} P_{qq}^{(0)} \otimes \Delta_{\bar{q}\bar{q}}^{(1)} - \frac{2}{\epsilon} P_{gg}^{(0)} \otimes \Delta_{\bar{q}\bar{q}}^{(1)} \\
&\quad - \frac{1}{\epsilon^2} P_{qq}^{(0)} \otimes P_{qq}^{(0)} \otimes \hat{\Delta}_{\bar{q}\bar{q}}^{(0)} \\
\Delta_{gg}^{(2)} &= \hat{\Delta}_{gg}^{(2)} - \Gamma_{\bar{q}\bar{q}}^{(1)} \otimes \hat{\Delta}_{\bar{q}\bar{q}}^{(0)} - \frac{1}{\epsilon} P_{qq}^{(0)} \otimes \Delta_{gg}^{(1)} - \frac{1}{\epsilon} P_{qq}^{(0)} \otimes \Delta_{\bar{q}\bar{q}}^{(1)} - \frac{1}{\epsilon} P_{gg}^{(0)} \otimes \Delta_{\bar{q}\bar{q}}^{(1)} \\
&\quad - \frac{1}{\epsilon^2} P_{qq}^{(0)} \otimes P_{qq}^{(0)} \otimes \hat{\Delta}_{\bar{q}\bar{q}}^{(0)} \\
\Delta_{gg}^{(2)} &= \hat{\Delta}_{gg}^{(2)} - \frac{4}{\epsilon} P_{qq}^{(0)} \otimes \Delta_{gg}^{(1)} - \frac{2}{\epsilon^2} P_{qq}^{(0)} \otimes P_{qq}^{(0)} \otimes \hat{\Delta}_{\bar{q}\bar{q}}^{(0)} \quad (30)
\end{aligned}$$

We have computed  $\hat{\Delta}_{ab}$  for all those reactions that contribute to scalar production to order  $a_s^2$  and substituted them into eqns.(29,30) to obtain finite partonic coefficient functions  $\Delta_{ab}$ . The results are lengthy and hence they are presented in the Appendix after setting  $\mu_R = \mu_F$ . It is straightforward to obtain the  $\mu_R$  dependence of the partonic coefficient functions presented in the Appendix using the RG equations given in eqns.(7). The mass factorisation implies DGLAP evolution equation:

$$\mu_F^2 \frac{d}{d\mu_F^2} f_a(x, \mu_F^2) = \frac{1}{2} \sum_b P_{ab} \left( x, \mu_F^2 \right) \otimes f_b(x, \mu_F^2), \quad (31)$$

where  $P_{ab}$  are Altarelli-Parisi splitting functions [36]. The DGLAP evolution equation determines the scale evolution of the parton densities appearing in eqn.(5). Note that the RG equations of strong, Yukawa couplings (eqn.(13)) along with the above DGLAP evolution equations (eqn.(31)) control both factorisation and renormalisation scale dependences of  $\Delta_{ab}$  at every order in perturbation theory.

We have made several checks on our NNLO results, both analytically as well as numerically. First and the foremost check is the observation of cancellation of all the poles in  $\epsilon$  that result from UV, soft and collinear divergences after all the appropriate renormalisation constants and factorisation kernels are systematically taken into account. The second check involves the comparison of our results against those computed for Higgs production through bottom quark annihilation [37]. Note that we have presented our results in such a way that they can be used for both neutral scalar (sneutrino) and charged scalar (sleptons) productions. So, the comparison against [37] is possible only after combining various pieces of the coefficient functions and then multiplying  $x$  and setting  $C_A = 3, C_F = 4/3, T_f = 1/2$  in our expressions. We found complete agreement with [37] which serves as an important check on our computation. Finally, we have reproduced all those plots given in [37] using our code in order to check the correctness of numerical code. In the next section we will discuss in detail the numerical impact of our results for both sneutrino and charged slepton productions at hadron colliders.

Recently, there have been several breakthroughs in understanding the structure of perturbative series to all orders in perturbation theory, thanks to explicit results on form factors and Altarelli-Parisi splitting functions (see [38–43]) to three loop level in QCD. The computation of such quantities reveals the long distance physics resulting from the soft gluon emissions in the scattering processes. The soft gluon contributions to hadronic cross sections often dominate over the rest in the region where the partonic scaling variable  $x$  approaches unity. Due to the peculiar behavior of the partonic fluxes in this region, often these effects need to be resummed to all orders in perturbation theory. Resummation of soft gluons for hadronic reactions can now be achieved upto next to next to leading logarithm ( $N^3LL$ ) level using the available three loop results (see [44–47]). More on the structure of perturbative results both in fixed order as well as in the resummed quantities can be found in [47–50]. In [47], soft gluon enhanced partonic contributions were obtained for Drell-Yan, Higgs productions at hadronic colliders. This was achieved by using the collinear factorisation property of scattering cross sections, the Sudakov resummation of soft gluon effects and applying various renormalisation group techniques. In [51], order  $\alpha_s^3$  soft gluon contributions to Higgs production through bottom quark annihilation process at hadron colliders were presented for the first time using the soft gluon enhanced cross sections thus obtained. Since the coupling of SM Higgs boson to bottom quarks and that of sneutrino/sleptons are both of Yukawa type, we can use  $\Delta_{bb}^{(3)}$  of [51] to study the soft gluon effects on the sneutrino and charged slepton production cross sections at hadron colliders. We will present the numerical impact of these effects towards the end of next section. Such a study presents a quantitative estimate on the missing higher order contributions to the processes under study.

### 3 Results and Discussion

Having obtained the compact analytic results for the partonic coefficient functions  $\Delta_{ab}$  for various subprocesses to NNLO in perturbative QCD, we now endeavor to study their impacts on the resonant production of sneutrino and charged slepton at the LHC ( $\sqrt{S} = 14$  TeV) and for the Run II of Tevatron ( $\sqrt{S} = 1.96$  TeV). As discussed in the Introduction, we will limit ourselves only to contributions from the first generation of quarks. Since at hadron colliders, the resonant production is through the interaction term  $\lambda'_{ijk} L_i Q_j D_k^c$  in the Lagrangian (see eq.(1)), for  $j, k = 2, 3$ , the production rate will be suppressed due to the low flux of the sea quarks. To obtain the production cross section to a particular order, one has to convolute the partonic coefficient functions  $\Delta_{ab}$  with the corresponding parton densities  $f_a$ , both to the same order. Further the coupling constants  $a_s(\mu_R)$  and  $\lambda'(\mu_R)$  should also be evaluated using the corresponding RGEs (eqn.(7)) computed to the same order.

Following the Ref [26], the solution to RGE (second equation in eq.(7)) for  $\lambda'(\mu_R^2)$  is given by ,

$$\lambda'(\mu_R^2) = \lambda'(\mu_0^2) \frac{C(a_s(\mu_R^2))}{C(a_s(\mu_0^2))} \quad (32)$$

with

$$C(a_s) = a_s^{A_0} \sum_{i=0}^{\infty} a_s^i C_i. \quad (33)$$

The  $C_i$  are given by

$$\begin{aligned} C_0 &= 1, & C_1 &= A_1, \\ C_2 &= \frac{1}{2}(A_1^2 + A_2), & C_3 &= \frac{1}{6}(A_1^3 + 3A_1A_2 + 2A_3), \end{aligned} \quad (34)$$

with

$$\begin{aligned} A_0 &= c_0, & A_1 &= c_1 - b_1 c_0, & A_2 &= c_2 - b_1 c_1 + c_0(b_1^2 - b_2), \\ A_3 &= c_3 - b_1 c_2 + c_1(b_1^2 - b_2) + c_0(b_1 b_2 - b_1(b_1^2 - b_2) - b_3), \end{aligned} \quad (35)$$

and

$$c_i = \frac{\gamma_i}{\beta_0}, \quad b_i = \frac{\gamma_i}{\beta_0}, \quad (36)$$

and  $\mu_0$  is some reference scale at which both  $a_s$  as well as  $\lambda'$  are known. We have numerically evaluated  $a_s(\mu_R^2)$  and  $\lambda'(\mu_R^2)$  to relevant order namely LO, NLO and NNLO by truncating the terms in the RHS of eqn.(13). We have used  $\lambda'(M_Z^2) = 0.01$  irrespective of flavor and mass of the sneutrino/charged slepton. We have used the latest MSTW parton densities [52] in our numerical code and the corresponding values of  $\alpha_s(M_Z)$  for LO, NLO and NNLO provided with the sets.

### 3.1 Sneutrino Production

The total sneutrino production cross section as function of its mass is plotted in fig. 11 for LHC (left panel) and Run II of Tevatron (right panel) energies. We have set the renormalisation scale to be the mass of the sneutrino,  $\mu_R = m_{\tilde{\nu}}$ . The pair of lines corresponds to the two extreme choices of factorisation scale:  $\mu_F = m_{\tilde{\nu}}$  (upper) and  $\mu_F = 0.1m_{\tilde{\nu}}$  (lower). The plots clearly demonstrate that the NNLO contributions reduce the factorisation scale dependence improving the theoretical predictions for sneutrino production cross section. To quantify the percentage variation with respect to the factorisation scale we define

$$\delta\sigma_I^\phi(\mu_F) = \frac{\sigma_I^\phi(\mu_F = \mu_R = m_{\tilde{\nu}}) - \sigma_I^\phi(\mu_F = 0.1m_{\tilde{\nu}}, \mu_R = m_{\tilde{\nu}})}{\sigma_I^\phi(\mu_F = \mu_R = m_{\tilde{\nu}})} \quad (37)$$

where  $I = LO, NLO, NNLO$ . The cross section falls off with the sneutrino mass due to

	Mass Range ( $m_{\tilde{\nu}}$ )	LO in %	NLO in %	NNLO in %
Tevatron	100 GeV to 1 TeV	-4.6 to 140	-2.2 to -39	-1.1 to -10.6
LHC	100 GeV to 450 GeV	40 to 2.3	23 to 1.8	9.3 to 1.1
	510 GeV to 1 TeV	-1.2 to -17	-0.22 to -5.2	-0.24 to -1.2

Table 2:  $\delta\sigma^{(i)}(\mu_F)$  in % in the mass range between 100 GeV and 1 TeV at Tevatron and LHC energies.

the availability of phase space with respect to the mass, the choice of  $\mu_R = m_{\tilde{\nu}}$  and the parton densities. The latter effect, understandably, is more pronounced at the Tevatron than at the LHC.

In order to estimate the magnitude of the QCD corrections at NLO and NNLO, we define the K-factors as follows:

$$K^{(1)} = \sigma_{\text{NLO}}^\phi / \sigma_{\text{LO}}^\phi \quad K^{(2)} = \sigma_{\text{NNLO}}^\phi / \sigma_{\text{LO}}^\phi.$$

In fig.12, we have plotted both  $K^{(i)}$  ( $i = 1, 2$ ) as a function of sneutrino mass. We have chosen  $\mu_F = \mu_R = m_{\tilde{\nu}}$  for this study. At the LHC, The  $K^{(1)}$  varies between 1.23 to 1.46 and  $K^{(2)}$  between 1.27 to 1.52 in the mass range  $100 \text{ GeV} \leq m \leq 1 \text{ TeV}$ . At the Tevatron, we find that  $K^{(1)}$  varies between 1.55 to 1.53 and  $K^{(2)}$  between 1.65 to 1.85 for the same mass range. Note that numbers for  $K^{(1)}$  differ slightly from those given in our earlier work [15] due to the running of  $\lambda'$  in the present analysis. We also observe that K factor is much bigger at the Tevatron compared to that of at the LHC. The reason behind this is attributed to the different behavior of parton densities at the Tevatron and the LHC. Note that parton densities rise steeply as  $x \rightarrow 0$  and fall off very fast as  $x \rightarrow 1$ , which means the dominant contribution to the production results from the phase space region where  $x \sim \tau (= m_{\tilde{\nu}}^2/S)$  becomes small.  $\tau$  at Tevatron ( $0.05 \lesssim \tau \lesssim 0.5$ ) is larger compared

to that at LHC ( $0.007 \lesssim \tau \lesssim 0.07$ ) (see also fig.12). Because of this, at Tevatron the valence quark initiated processes dominate while gluon and sea quark initiated processes dominate at the LHC. As the mass of the sneutrino increases, that is  $x$  approaches to unity, the  $K$ -factor at Tevatron naturally falls off. At LHC, in the higher mass region ( $\sim 1$  TeV), valence quark densities start to dominate and hence it stays almost flat compared to Tevatron. We find that the most dominant sub processes are the  $d\bar{d}$  and  $dg$  initiated processes. The  $dg$  sub process which begins at NLO gives a negative contribution both at NLO and NNLO.

We now turn to study the impact of the factorisation scale ( $\mu_F$ ) and the renormalisation scale ( $\mu_R$ ) on the production cross section. The factorisation scale dependence for both LHC (left panel) and Tevatron (right panel) are shown in upper panels of fig. 13, for  $m_{\tilde{\nu}} = 300 \text{ GeV}$  (LHC),  $m_{\tilde{\nu}} = 120 \text{ GeV}$  (Tevatron). We have chosen  $\mu_R = m_{\tilde{\nu}}$  for both the LHC and the Tevatron. The factorisation scale is varied between  $\mu_F = 0.1 m_{\tilde{\nu}}$  and  $\mu_F = 10 m_{\tilde{\nu}}$ . We find that the factorisation scale dependence decreases in going from LO to NLO to NNLO as expected.

The dependence of the renormalisation scale dependence on the total cross sections for the resonant production of sneutrino at the LHC and the Tevatron is shown in the lower panels of fig. 13. Note that the LO is already  $\mu_R$  dependent due to the coupling  $\lambda'(\mu_R)$ . We have performed this analysis for sneutrino mass  $m_{\tilde{\nu}} = 300 \text{ GeV}$  (LHC),  $m_{\tilde{\nu}} = 120 \text{ GeV}$  (Tevatron). We have set the factorisation scale  $\mu_F = m_{\tilde{\nu}}/4$  (see for example, Ref. [53] for more details) and the renormalisation scale is varied in the range  $0.1 \leq \mu_R/m_{\tilde{\nu}} \leq 10$ . We find significant reduction in the  $\mu_R$  scale dependence when higher order QCD corrections are included. It is clear from both the panels of fig. 13 that our present NNLO result makes the predictions almost independent of both factorisation and renormalisation scales.

### 3.2 Charged slepton production

We now study the numerical impact of our NNLO results on the charged slepton production for both Tevatron and LHC energies. In fig. 14, we have plotted the total cross section as function of charged slepton mass. The upper (lower) set of lines corresponds to the factorisation scale  $\mu_F = m_{\tilde{\ell}^+} (0.1m_{\tilde{\ell}^+})$ . The improvement due to NLO and NNLO pieces is evident. As we expect the  $K$ -factors (see figs.15) are quite similar to the case of neutral scalar production. In upper panels of fig. (16), we have shown the production cross section as a function of factorisation scale  $\mu_F$  for the slepton mass  $m_{\tilde{\ell}^+} = 300 \text{ GeV}$  (LHC),  $m_{\tilde{\ell}^+} = 120 \text{ GeV}$  (Tevatron) and fixed the renormalisation scale at  $\mu_R = m_{\tilde{\ell}^+}$ . In the lower panels of fig. (16), we have shown  $\mu_R$  variation for the LHC and the Tevatron. We have done this for charged slepton mass  $m_{\tilde{\ell}^+} = 300 \text{ GeV}$  (LHC),  $m_{\tilde{\ell}^+} = 120 \text{ GeV}$  (Tevatron) and fixed the factorisation scale  $\mu_F = \frac{1}{4} m_{\tilde{\ell}^+}$  (see Ref. [53]). We again find that the scale dependence gets reduced significantly as we include higher order terms in the perturbative expansion. Our numerical code can also produce results for  $\tilde{\ell}^-$  production both at the LHC and the Tevatron. At Tevatron, the production rates for  $\tilde{\ell}^-$  is found to be same as that of  $\tilde{\ell}^+$  because the contributing fluxes and the partonic coefficient func-

tions are identical. At the LHC, this is not the case because of different fluxes that contribute for  $\tilde{\ell}^+$  and  $\tilde{\ell}^-$ .

### 3.3 Soft gluon contributions at order $\alpha_s^3$

The order  $\alpha_s^3$  partonic coefficient function  $\Delta_{bb}^{(3)}$  resulting from the soft gluons is known for the Higgs boson production through  $b\bar{b}$  annihilation (see [51]). The same coefficient function can be used here to study the impact of soft gluons for the sneutrino (also for the charged slepton) production at  $\alpha_s^3$  level due to identical structure of the interaction terms responsible for their production mechanisms. For our numerical study, we have used the available three loop  $\beta_3$  and  $\gamma_3$  to evolve  $\alpha_s$  and  $\lambda'$  respectively. For parton density sets, we can only use the available NNLO evolved MSTW 2008 sets. In fig. (17), we have plotted the  $N^3LO$  corrected sneutrino production cross sections against its mass (upper panels) and the renormalisation scale (lower panels) on for both LHC as well as Tevatron energies. While the order  $\alpha_s^3$  soft gluon effects to the production of sneutrinos is indistinguishable with respect to exact  $NNLO$  contributions, it reduces the uncertainty resulting from the choice of renormalisation scale significantly.

## 4 Conclusions

The ongoing program in search of signals of BSM scenarios can be successful only if the theory predictions are precise and reliable. In this paper we have attempted to make predictions for the production of sneutrinos and sleptons at hadron colliders such as Tevatron and the LHC. The resonant production of sneutrinos and sleptons are possible at these colliders thanks to  $R$ -parity violating interactions present in the supersymmetric theory which is one of the most studied BSM in the literature. Often predictions based on subprocess contributions computed at leading order in perturbation theory suffer from uncertainties resulting from the arbitrariness in the choice of renormalisation and factorisation scales. These scales are artifacts of the perturbation theory and hence are unphysical. The sensitivity to these scales signals the missing higher order contributions that need to be included in order to make the predictions reliable. In other words, contributions from NLO and NNLO sub processes are expected to reduce these theoretical uncertainties. In addition, the potential SM background processes to resonant production of sneutrinos and sleptons and their subsequent decays are well under control as they are known to NNLO level in QCD. Hence, we have computed all the subprocess contributions to the production cross sections for sneutrino and sleptons upto order  $\alpha_s^2$  (i.e., NNLO) in perturbative QCD. We have used dimensional regularisation to regulate UV, soft and collinear divergences. The renormalisation and the factorisation are done in  $\overline{MS}$  scheme. We have used the latest parton density sets provided by MSTW for all our analysis. We have demonstrated how the inclusion of NNLO contributions can reduce the scale uncertainties over wide range of sneutrino and slepton masses for both Tevatron and LHC energies. We also find significant increase in the cross section due to opening up of several

new partonic channels beyond the leading order. The increase in the cross section due to the inclusion of NNLO contributions compared to that of NLO is found to be 6.6% to 21% for Tevatron and 3.4% to 4% for LHC and the total NNLO K factor varies from 1.65 to 1.85 for Tevatron and 1.27 to 1.52 for LHC in the mass range of 100 GeV to 1 TeV. In order to estimate the impact of QCD corrections beyond NNLO, we have performed an analysis taking into account the dominant soft gluon contributions at  $N^3LO$  and found that they are stable under perturbation. The calculations presented in this paper are not particular to supersymmetric theories, but can be applied to any color-singlet scalar (pseudoscalar) coupling to a quark anti-quark pair.

## Acknowledgements

The work of V.R. has been partially supported by funds made available to the Regional Centre for Accelerator based Particle Physics (RECAPP) by the Department of Atomic Energy, Govt. of India. We would like to thank the cluster computing facility at Harish-Chandra Research Institute where part of computational work for this study was carried out. S.M would like to thank RECAPP center for his visit, where part of the work was done.



## 5 Appendix

The leading order contribution (fig.(1)) from the subprocess  $q_i + \bar{q}_j \rightarrow \phi$  gives:

$$\hat{\Delta}_{q\bar{q}}^{(0)} = \Delta_{q\bar{q}}^{(0)} = \delta(1-x) \quad (38)$$

To order  $a_s$ , we need to include  $q_i + \bar{q}_j \rightarrow g + \phi$ ,  $q_i(\bar{q}_i) + g \rightarrow q_j(\bar{q}_j) + \phi$  and one loop corrections to  $q_i + \bar{q}_j \rightarrow \phi$ . The quark anti-quark initiated processes (fig.(2,3)) give

$$\begin{aligned} \Delta_{q\bar{q}}^{(1)} &= C_F \left[ 2 - 2x + \ln(x) \left\{ 2 - \frac{4}{(1-x)} + 2x \right\} + \ln(1-x) \{-4 - 4x\} \right. \\ &\quad \left. + 8 \left( \frac{\ln(1-x)}{(1-x)} \right)_+ + \ln \left( \frac{m_\phi^2}{\mu_F^2} \right) \left\{ -2 + \frac{4}{(1-x)_+} - 2x \right\} + \delta(1-x) \{-2 + 4\zeta_2\} \right] \\ &\quad + \epsilon C_F \left[ \left( -\frac{3}{(1-x)_+} \zeta_2 + \frac{3}{2} \zeta_2 + \frac{3}{2} x \zeta_2 \right) + \ln(x) \{-1 + x\} \right. \\ &\quad \left. + \ln^2(x) \left\{ -\frac{1}{2} + \frac{1}{(1-x)} - \frac{1}{2}x \right\} + \ln(1-x) \left\{ 2 - 2x + \ln(x) \right. \right. \\ &\quad \left. \left. \times \left( 2 - \frac{4}{(1-x)} + 2x \right) \right\} + \ln^2(1-x) \{-2 - 2x\} + 4 \left( \frac{\ln^2(1-x)}{(1-x)} \right)_+ \right. \\ &\quad \left. + \ln \left( \frac{m_\phi^2}{\mu_F^2} \right) \left\{ 1 - x + \ln(x) \left( 1 - \frac{2}{(1-x)} + x \right) + \ln(1-x) (-2 - 2x) \right. \right. \\ &\quad \left. \left. + 4 \left( \frac{\ln(1-x)}{(1-x)} \right)_+ \right\} + \ln^2 \left( \frac{m_\phi^2}{\mu_F^2} \right) \left\{ -\frac{1}{2} + \frac{1}{(1-x)_+} - \frac{1}{2}x \right\} \right. \\ &\quad \left. + \delta(1-x) \left\{ 2 + \ln \left( \frac{m_\phi^2}{\mu_F^2} \right) (-1 + 2\zeta_2) \right\} \right] \quad (39) \end{aligned}$$

and quark (anti-quark) gluon initiated processes (fig.(4)) give

$$\begin{aligned} \Delta_{qg}^{(1)} &= \Delta_{\bar{q}g}^{(1)} \\ &= T_f \left[ -\frac{3}{2} + 5x - \frac{7}{2}x^2 + \ln(x) \{-1 + 2x - 2x^2\} \right. \\ &\quad \left. + \ln(1-x) \{2 - 4x + 4x^2\} + \ln \left( \frac{m_\phi^2}{\mu_F^2} \right) \{1 - 2x + 2x^2\} \right] \\ &\quad + \epsilon T_f \left[ \frac{3}{2} - \frac{3}{4}\zeta_2 - 5x + \frac{3}{2}x\zeta_2 + \frac{7}{2}x^2 - \frac{3}{2}x^2\zeta_2 + \ln(x) \left\{ \frac{3}{4} - \frac{5}{2}x + \frac{7}{4}x^2 \right\} \right] \end{aligned}$$

$$\begin{aligned}
& + \ln^2(x) \left\{ \frac{1}{4} - \frac{1}{2}x + \frac{1}{2}x^2 \right\} + \ln(1-x) \left\{ -\frac{3}{2} + 5x - \frac{7}{2}x^2 \right. \\
& \left. + \ln(x) \left( -1 + 2x - 2x^2 \right) \right\} + \ln^2(1-x) \left\{ 1 - 2x + 2x^2 \right\} \\
& + \ln\left(\frac{m_\phi^2}{\mu_F^2}\right) \left\{ -\frac{3}{4} + \frac{5}{2}x - \frac{7}{4}x^2 + \ln(x) \left( -\frac{1}{2} + x - x^2 \right) \right. \\
& \left. + \ln(1-x) \left( 1 - 2x + 2x^2 \right) \right\} + \ln^2\left(\frac{m_\phi^2}{\mu_F^2}\right) \left\{ \frac{1}{4} - \frac{1}{2}x + \frac{1}{2}x^2 \right\} \quad (40)
\end{aligned}$$

In the above results we have presented results to order  $\epsilon$  that will contribute to NNLO results.

To order  $a_s^2$ , several partonic subprocesses contribute. We present the contributions coming from each subprocess below. The quark anti-quark initiated processes with no gluon (fig.(5)), one gluon (fig.(6)) and two gluons (fig.(7)) in the final state along with  $\phi$  constitute a sub class giving order  $a_s^2$  contribution. This class consists of processes with two loop corrections to leading order  $q_i + \bar{q}_j \rightarrow \phi$  (no gluon) along with one loop corrections to  $q_i + \bar{q}_j \rightarrow \phi + g$  (one gluon). In addition we have  $q_i + \bar{q}_j \rightarrow g + g + \phi$  (two gluons) in this class. The unrenormalised form factor  $\mathcal{F}_\phi$  upto two loop order (fig.(5)) is found to be [51]

$$\begin{aligned}
\mathcal{F}_\phi(m_\phi^2, \mu^2) &= 1 + \hat{a}_s \left( -\frac{m_\phi^2}{\mu^2} \right)^{\frac{\epsilon}{2}} S_\epsilon C_F \left\{ -\frac{8}{\epsilon^2} - 2 + \zeta_2 + \epsilon \left( 2 - \frac{7}{3}\zeta_3 \right) + \epsilon^2 \left( -2 + \frac{1}{4}\zeta_2 \right. \right. \\
& \left. \left. + \frac{47}{80}\zeta_2^2 \right) \right\} + \hat{a}_s^2 \left( -\frac{m_\phi^2}{\mu^2} \right)^\epsilon S_\epsilon^2 \left[ C_A C_F \left\{ -\frac{1655}{81} + \frac{44}{3\epsilon^3} + \frac{4}{\epsilon^2}\zeta_2 - \frac{134}{9\epsilon^2} \right. \right. \\
& \left. \left. + \frac{11}{3\epsilon}\zeta_2 - \frac{26}{\epsilon}\zeta_3 + \frac{440}{27\epsilon} - \frac{103}{18}\zeta_2 + \frac{44}{5}\zeta_2^2 + \frac{305}{9}\zeta_3 \right\} + n_f C_F \left\{ \frac{416}{81} - \frac{8}{3\epsilon^3} \right. \right. \\
& \left. \left. + \frac{20}{9\epsilon^2} - \frac{2}{3\epsilon}\zeta_2 - \frac{92}{27\epsilon} + \frac{5}{9}\zeta_2 - \frac{26}{9}\zeta_3 \right\} + C_F^2 \left\{ 22 + \frac{32}{\epsilon^4} - \frac{8}{\epsilon^2}\zeta_2 + \frac{16}{\epsilon^2} \right. \right. \\
& \left. \left. - \frac{12}{\epsilon}\zeta_2 + \frac{128}{3\epsilon}\zeta_3 - \frac{16}{\epsilon} + 12\zeta_2 - 13\zeta_2^2 - 30\zeta_3 \right\} \right] \quad (41)
\end{aligned}$$

The contributions from quark antiquark annihilation processes can be split into two parts: contributions coming from threshold region called soft plus virtual (S+V) contribution:

$$\begin{aligned}
\Delta_{q\bar{q}}^{(2),S+V} &= n_f C_F \left[ \frac{32}{3}\mathcal{D}_2(x) - \frac{160}{9}\mathcal{D}_1(x) + \frac{224}{27}\mathcal{D}_0(x) - \frac{32}{3}\mathcal{D}_0(x)\zeta_2 \right. \\
& \left. + \ln\left(\frac{m_\phi^2}{\mu_F^2}\right) \left\{ \frac{32}{3}\mathcal{D}_1(x) - \frac{80}{9}\mathcal{D}_0(x) \right\} + \ln^2\left(\frac{m_\phi^2}{\mu_F^2}\right) \left\{ \frac{8}{3}\mathcal{D}_0(x) \right\} \right]
\end{aligned}$$

$$\begin{aligned}
& +\delta(1-x)\left\{\frac{8}{9}+8\zeta_3-\frac{40\zeta_2}{9}\right\}+C_F^2\left[128\mathcal{D}_3(x)-64\mathcal{D}_1(x)-128\mathcal{D}_1(x)\zeta_2\right. \\
& +256\mathcal{D}_0(x)\zeta_3+\ln\left(\frac{m_\phi^2}{\mu_F^2}\right)\left\{192\mathcal{D}_2(x)-32\mathcal{D}_0(x)-64\mathcal{D}_0(x)\zeta_2\right\} \\
& +\ln^2\left(\frac{m_\phi^2}{\mu_F^2}\right)\left\{64\mathcal{D}_1(x)\right\}+\delta(1-x)\left(16-60\zeta_3+\frac{8}{5}\zeta_2^2+\ln\left(\frac{m_\phi^2}{\mu_F^2}\right)\left\{176\zeta_3\right. \right. \\
& \left. \left.-24\zeta_2\right\}+\ln^2\left(\frac{m_\phi^2}{\mu_F^2}\right)\left\{-32\zeta_2\right\}\right)+C_A C_F\left[-\frac{176}{3}\mathcal{D}_2(x)+\frac{1072}{9}\mathcal{D}_1(x)\right. \\
& \left.-32\mathcal{D}_1(x)\zeta_2-\frac{1616}{27}\mathcal{D}_0(x)+56\mathcal{D}_0(x)\zeta_3+\frac{176}{3}\mathcal{D}_0(x)\zeta_2+\ln\left(\frac{m_\phi^2}{\mu_F^2}\right)\right. \\
& \left.\times\left\{-\frac{176}{3}\mathcal{D}_1(x)+\frac{536}{9}\mathcal{D}_0(x)-16\mathcal{D}_0(x)\zeta_2\right\}+\ln^2\left(\frac{m_\phi^2}{\mu_F^2}\right)\left\{-\frac{44}{3}\mathcal{D}_0(x)\right\}\right. \\
& \left.+\delta(1-x)\left(\frac{166}{9}-8\zeta_3+\frac{232}{9}\zeta_2-\frac{12}{5}\zeta_2^2+\ln\left(\frac{m_\phi^2}{\mu_F^2}\right)\left\{-12-24\zeta_3\right\}\right)\right] \quad (42)
\end{aligned}$$

where the "plus" distributions  $\mathcal{D}_i(x)$  are given by

$$\mathcal{D}_i(x) = \left(\frac{\log^i(1-x)}{1-x}\right)_+$$

and the hard contribution whose  $C_A C_F$  part is given by

$$\begin{aligned}
\Delta_{q\bar{q}}^{(2),C_A} & = C_A C_F \left[ \frac{1186}{27} - 28\zeta_3 - \frac{100}{3}\zeta_2 + \frac{430}{27}x - 28x\zeta_3 - \frac{76}{3}x\zeta_2 \right. \\
& + S_{1,2}(1-x) \left\{ 4 - \frac{8}{(1-x)} + 4x \right\} + Li_3(1-x) \left\{ 12 - \frac{24}{(1-x)} + 12x \right\} \\
& + Li_2(1-x) \left\{ -16 + \frac{8}{3(1-x)} - 4x \right\} + \ln(x) \left\{ 40 - \frac{232}{3(1-x)} \right. \\
& \left. + \frac{16}{(1-x)}\zeta_2 - 8\zeta_2 + \frac{154}{3}x - 8x\zeta_2 \right\} + \ln(x) Li_2(1-x) \left\{ -8 \right. \\
& \left. + \frac{16}{(1-x)} - 8x \right\} + \ln^2(x) \left\{ \frac{59}{3} - \frac{29}{(1-x)} + \frac{65}{3}x \right\} + \ln(1-x) \\
& \times \left\{ -\frac{416}{9} + 16\zeta_2 - \frac{692}{9}x + 16x\zeta_2 \right\} + \ln(1-x) Li_2(1-x)
\end{aligned}$$

$$\begin{aligned}
& \times \left\{ 8 - \frac{16}{(1-x)} + 8x \right\} + \ln(1-x) \ln(x) \left\{ -\frac{176}{3} + \frac{280}{3(1-x)} - \frac{176}{3}x \right\} \\
& + \ln^2(1-x) \left\{ \frac{88}{3} + \frac{88}{3}x \right\} + \ln\left(\frac{m_\phi^2}{\mu_F^2}\right) \left( \left\{ -\frac{208}{9} + 8\zeta_2 - \frac{364}{9}x + 8x\zeta_2 \right\} \right. \\
& + Li_2(1-x) \left\{ 8 - \frac{16}{(1-x)} + 8x \right\} + \ln(x) \left\{ -\frac{88}{3} + \frac{140}{3(1-x)} - \frac{88}{3}x \right\} \\
& \left. + \ln(1-x) \left\{ \frac{88}{3} + \frac{88}{3}x \right\} \right) + \ln^2\left(\frac{m_\phi^2}{\mu_F^2}\right) \left\{ \frac{22}{3} + \frac{22}{3}x \right\} \quad (43)
\end{aligned}$$

and the  $C_F^2$  part is given by

$$\begin{aligned}
\Delta_{q\bar{q}}^{(2),C_F} &= C_F^2 \left[ -72 - 128\zeta_3 + 96\zeta_2 + 64x - 128x\zeta_3 - 96x\zeta_2 + S_{1,2}(1-x) \right. \\
& \times \left( 80 - \frac{64}{(1-x)} + 80x \right) + Li_3(1-x) \left( -64 - \frac{16}{(1-x)} - 64x \right) \\
& + Li_2(1-x)(-24 - 16x) + \ln(x) \left\{ -56 + \frac{32}{(1-x)} + \frac{128}{(1-x)}\zeta_2 \right. \\
& \left. - 96\zeta_2 - 96x\zeta_2 + Li_2(1-x) \left( 32 - \frac{48}{(1-x)} + 32x \right) \right\} \\
& + \ln^2(x) \{-8 + 16x\} + \ln^3(x) \left\{ \frac{58}{3} - \frac{24}{(1-x)} + \frac{58}{3}x \right\} + \ln(1-x) \\
& \times \left\{ 80 + 64\zeta_2 - 4x + 64x\zeta_2 + Li_2(1-x) \left( 40 + \frac{48}{(1-x)} + 40x \right) \right. \\
& \left. + \ln(x) \{24 - 56x\} + \ln^2(x) \left( -96 + \frac{144}{(1-x)} - 96x \right) \right\} + \ln^2(1-x) \\
& \times \left\{ (-32 + 32x) + \ln(x) \left( 156 - \frac{248}{(1-x)} + 156x \right) \right\} \\
& + \ln^3(1-x) \{-64 - 64x\} + \ln\left(\frac{m_\phi^2}{\mu_F^2}\right) \left\{ 40 + 32\zeta_2 + 32x\zeta_2 + Li_2(1-x) \right. \\
& \times \left( 16 + \frac{32}{(1-x)} + 16x \right) + \ln(x) \{16 - 32x\} + \ln^2(x) \left\{ -36 + \frac{48}{(1-x)} \right. \\
& \left. \left. - 36x \right\} + \ln(1-x) \{-32 + 32x\} + \ln(1-x) \ln(x) \left\{ 144 - \frac{224}{(1-x)} \right. \right.
\end{aligned}$$

$$\begin{aligned}
& +144x \left. \right\} + \ln^2(1-x)(-96-96x) \left. \right\} + \ln^2\left(\frac{m_\phi^2}{\mu_F^2}\right) \left\{ -16 + 16x \right. \\
& \left. + \ln(x) \left\{ 24 - \frac{32}{(1-x)} + 24x \right\} + \ln(1-x)(-32-32x) \right\} \left. \right] \quad (44)
\end{aligned}$$

The functions  $S_{np}$  and  $Li_n$  are Nielsen integral and polylogarithm respectively:

$$\begin{aligned}
S_{np}(x) &= \frac{(-1)^{n+p-1}}{(n-1)! p!} \int_0^1 dz \frac{\log^{n-1}(z) \log^p(1-xz)}{z}, \\
Li_n(x) &= S_{n-1,1}(x), \quad \zeta_s = \sum_{n=1}^{\infty} n^{-s} \quad (45)
\end{aligned}$$

and for  $s = 2, 3$ , we have  $\zeta_2 = \pi^2/6, \zeta_3 = 1.202056903159 \dots$ . In addition, quark anti-quark pair in the initial and final states along with  $\phi$  (A and B in fig. (8)) and quark (anti-quark) quark (anti-quark) pair in the final state with  $\phi$  also arise at order  $a_s^2$  (C and D in fig. (9)). The contributions coming from the later will depend on whether we have identical quarks (anti-quarks) or non-identical quarks (anti-quarks). We present their contributions below along with various allowed interferences.

The  $s$ -channel processes (A in fig.(8)) with  $\phi$  emitted from incoming partons give

$$\begin{aligned}
\Delta_{q\bar{q}}^{(2),A\bar{A}} &= n_f C_F \left[ -\frac{4}{27} + \frac{16}{3}\zeta_2 - \frac{220}{27}x + \frac{16}{3}x\zeta_2 + Li_2(1-x) \left( -\frac{8}{3(1-x)} \right) \right. \\
& + \ln(x) \left\{ -4 + \frac{40}{3(1-x)} - \frac{28}{3}x \right\} + \ln^2(x) \left\{ -\frac{14}{3} + \frac{8}{(1-x)} - \frac{14}{3}x \right\} \\
& + \ln(1-x) \left\{ \frac{32}{9} + \frac{128}{9}x + \ln(x) \left( \frac{32}{3} - \frac{64}{3(1-x)} + \frac{32}{3}x \right) \right\} \\
& + \ln^2(1-x) \left\{ -\frac{16}{3} - \frac{16}{3}x \right\} + \ln\left(\frac{m_\phi^2}{\mu_F^2}\right) \left\{ \frac{16}{9} + \frac{64}{9}x + \ln(x) \right. \\
& \times \left( \frac{16}{3} - \frac{32}{3(1-x)} + \frac{16}{3}x \right) + \ln(1-x) \left( -\frac{16}{3} - \frac{16}{3}x \right) \left. \right\} \\
& \left. + \ln^2\left(\frac{m_\phi^2}{\mu_F^2}\right) \left\{ -\frac{4}{3} - \frac{4}{3}x \right\} \right] \quad (46)
\end{aligned}$$

The interference of  $s$ -channel processes (A in fig.(8)) with  $\phi$  emitted from incoming partons and  $t$ -channel processes (C and D in fig.(9)) give

$$\begin{aligned}
\Delta_{q\bar{q}}^{(2),A\bar{C}} &= \Delta_{q\bar{q}}^{(2),A\bar{D}} \\
&= \left( C_F - \frac{C_A}{2} \right) C_F \left[ 94 - 86x + S_{1,2}(1-x) \left( 28 - \frac{72}{(1-x)} + 28x \right) \right]
\end{aligned}$$

$$\begin{aligned}
& +Li_3(1-x) \left( -16 + \frac{32}{(1-x)} - 16x \right) + Li_2(1-x) \left( -32 - \frac{12}{(1-x)} \right. \\
& \left. -24x \right) + \ln(x) \left\{ 36 + \frac{16}{(1-x)} - 30x + Li_2(1-x) \left( 8 - \frac{24}{(1-x)} \right. \right. \\
& \left. \left. +8x \right) \right\} + \ln^2(x) \left\{ -2 + \frac{15}{(1-x)} + 2x \right\} + \ln^3(x) \left\{ -\frac{10}{3} + \frac{16}{3(1-x)} \right. \\
& \left. -\frac{10}{3}x \right\} + \ln(1-x) \left\{ -64 + 56x + Li_2(1-x) \left( 16 - \frac{32}{(1-x)} + 16x \right) \right. \\
& \left. + \ln(x) \left( -16 - \frac{24}{(1-x)} - 16x \right) + \ln^2(x) \left( 8 - \frac{16}{(1-x)} + 8x \right) \right\} \\
& + \ln \left( \frac{m_\phi^2}{\mu_F^2} \right) \left\{ -32 + 28x + Li_2(1-x) \left( 8 - \frac{16}{(1-x)} + 8x \right) \right. \\
& \left. + \ln(x) \left( -8 - \frac{12}{(1-x)} - 8x \right) + \ln^2(x) \left( 4 - \frac{8}{(1-x)} + 4x \right) \right\} \Big] \quad (47)
\end{aligned}$$

The  $s$ -channel processes (B in fig.(8)) with  $\phi$  emitted from outgoing partons give

$$\begin{aligned}
\Delta_{q\bar{q}}^{((2),B\bar{B})} &= C_F T_f \left[ -\frac{16}{3} + \frac{64}{3}x - 16x^2 - \frac{16}{3}x^2\zeta_2 + Li_2(-x) \left( -\frac{32}{3}x^2 \right) \right. \\
& \left. + \ln(x) \left\{ -\frac{8}{3} + \frac{16}{3}x + 8x^2 \right\} + \ln^2(x) \left\{ \frac{8}{3}x^2 \right\} \right. \\
& \left. + \ln(1+x) \ln(x) \left\{ -\frac{32}{3}x^2 \right\} \right] \quad (48)
\end{aligned}$$

The interference of  $s$ -channel processes (B in fig.(8)) with  $\phi$  emitted from outgoing partons and  $t$ -channel processes (C and D in fig.(9)) give

$$\begin{aligned}
\Delta_{q\bar{q}}^{(2),B\bar{C}} &= \Delta_{q\bar{q}}^{(2),B\bar{D}} \\
&= \left( C_F - \frac{C_A}{2} \right) C_F \left[ -6 - 4\zeta_2 + 32x + 8x\zeta_2 - 26x^2 + S_{1,2}(-x) \left( -48x^2 \right) \right. \\
& + S_{1,2}(1-x) \left( 32x^2 \right) + Li_3(-x) \left( -8x^2 \right) + Li_2(-x) \left( -8 + 16x \right) \\
& + Li_2(1-x) \left( -8 + 32x - 24x^2 \right) + \ln(x) \left\{ -8 + 28x + 8x^2\zeta_2 \right. \\
& \left. + Li_2(-x) \left( 24x^2 \right) + Li_2(1-x) \left( 16x^2 \right) \right\} + \ln^2(x) \left\{ -2 + 12x - 12x^2 \right\}
\end{aligned}$$

$$\begin{aligned}
& + \ln^3(x) \left\{ \frac{4}{3} x^2 \right\} + \ln(1+x) \left\{ -24x^2 \zeta_2 + Li_2(-x) (-48x^2) \right. \\
& \left. + \ln(x) (-8 + 16x) + \ln^2(x) (20x^2) \right\} + \ln^2(1+x) \ln(x) \left\{ -24x^2 \right\} \Big] (49)
\end{aligned}$$

For charged scalar production, only part of  $t$ -channel processes (C or D in fig.(9)) interfere with  $s$ -channel processes in of (A and B in fig.(8)), that is, either  $(\Delta_{q\bar{q}}^{(2),A\bar{C}}, \Delta_{q\bar{q}}^{(2),B\bar{C}})$  or  $(\Delta_{q\bar{q}}^{(2),A\bar{D}}, \Delta_{q\bar{q}}^{(2),B\bar{D}})$  will contribute.

To order  $a_s^2$ , quark (anti-quark) gluon initiated processes also receive contributions namely from one loop contributions to  $q_i(\bar{q}_i) + g \rightarrow q_i(\bar{q}_j) + \phi$  and processes involving an additional gluon in the final state,  $q_i(\bar{q}_i) + g \rightarrow q_i(\bar{q}_j) + g + \phi$ . This contribution is found to be  $\Delta_{qg}^{(2)} = \Delta_{\bar{q}g}^{(2)} = \Delta_{q(\bar{q})g}^{(2),C_A} + \Delta_{q(\bar{q})g}^{(2),C_F}$ , where

$$\begin{aligned}
\Delta_{q(\bar{q})g}^{(2),C_A} &= C_A T_f \left[ \frac{395}{9} - \frac{208}{27x} - \frac{32}{3x} \zeta_2 - 4\zeta_3 + 16\zeta_2 - \frac{866}{9}x - 16x\zeta_3 - 80x\zeta_2 \right. \\
& + \frac{1513}{27}x^2 - 8x^2\zeta_3 + \frac{320}{3}x^2\zeta_2 + Li_3\left(\frac{1-x}{1+x}\right) (16 + 32x + 32x^2) \\
& + Li_3\left(-\frac{1-x}{1+x}\right) (-16 - 32x - 32x^2) + S_{1,2}(1-x) (32 + 96x + 32x^2) \\
& + Li_3(-x) (-8 - 16x - 16x^2) + Li_3(1-x) (-56 - 144x - 48x^2) \\
& + Li_2(-x) (12 + 32x + 20x^2) + Li_2(1-x) \left( -16 + \frac{64}{3x} + 64x \right. \\
& \left. + \frac{212}{3}x^2 \right) + \ln(x) \left\{ \frac{68}{3} - \frac{44}{3}x - 80x\zeta_2 - \frac{1130}{9}x^2 + 32x^2\zeta_2 \right. \\
& \left. + Li_2(-x) (16 + 32x + 32x^2) + Li_2(1-x) (-16 + 32x - 16x^2) \right\} \\
& + \ln^2(x) \left\{ -1 + 36x - \frac{292}{3}x^2 \right\} + \ln^3(x) \left\{ \frac{10}{3} + \frac{28}{3}x \right\} + \ln(1+x) \\
& \times \left\{ \ln(x) (12 + 32x + 20x^2) + \ln^2(x) (12 + 24x + 24x^2) \right\} \\
& + \ln(1-x) \left\{ -\frac{152}{3} + \frac{32}{9x} - 32\zeta_2 + \frac{38}{3}x + 32x\zeta_2 + \frac{364}{9}x^2 - 64x^2\zeta_2 \right. \\
& \left. + Li_2(-x) (-16 - 32x - 32x^2) + Li_2(1-x) (52 + 88x + 40x^2) \right\}
\end{aligned}$$

$$\begin{aligned}
& + \ln(x) (4 - 112x + 248x^2) + \ln^2(x) (-12 - 56x + 8x^2) \\
& + \ln(1+x) \ln(x) (-16 - 32x - 32x^2) \Big\} + \ln^2(1-x) \left\{ -10 + \frac{32}{3x} \right. \\
& + 96x - \frac{290}{3}x^2 + \ln(x) (4 + 88x - 24x^2) \Big\} + \ln^3(1-x) \left\{ \frac{26}{3} - \frac{52}{3}x \right. \\
& + \left. \frac{52}{3}x^2 \right\} + \ln\left(\frac{m_\phi^2}{\mu_F^2}\right) \left\{ -\frac{82}{3} + \frac{16}{9x} - 16\zeta_2 + \frac{16}{3}x + 16x\zeta_2 + \frac{218}{9}x^2 \right. \\
& - 32x^2\zeta_2 + Li_2(-x) (-8 - 16x - 16x^2) + Li_2(1-x) (24 + 48x \\
& + 16x^2) + \ln(x) (-4 - 40x + 112x^2) + \ln^2(x) (-8 - 24x) \\
& + \ln(1+x) \ln(x) (-8 - 16x - 16x^2) + \ln(1-x) \left( -4 + \frac{32}{3x} + 88x \right. \\
& - \left. \frac{284}{3}x^2 \right) + \ln(1-x) \ln(x) (8 + 80x - 16x^2) + \ln^2(1-x) (12 - 24x \\
& + 24x^2) \Big\} + \ln^2\left(\frac{m_\phi^2}{\mu_F^2}\right) \left\{ 2 + \frac{8}{3x} + 16x - \frac{62}{3}x^2 + \ln(x) (4 + 16x) \right. \\
& \left. + \ln(1-x) (4 - 8x + 8x^2) \right\} \Big] \tag{50}
\end{aligned}$$

and

$$\begin{aligned}
& \Delta_{q(\bar{q})g}^{(2),CF} \\
& = C_F T_f \left[ -\frac{129}{2} + 76\zeta_3 + 20\zeta_2 + 329x - 152x\zeta_3 - 64x\zeta_2 - \frac{549}{2}x^2 \right. \\
& + 200x^2\zeta_3 + 24x^2\zeta_2 + S_{1,2}(1-x) (-28 + 56x - 136x^2) \\
& + Li_3(-x) (64x^2) + Li_3(1-x) (-12 + 24x + 72x^2) \\
& + Li_2(-x) (-8 - 32x - 24x^2) + Li_2(1-x) (-26 - 32x + 56x^2) \\
& + \ln(x) \left\{ -35 + 16\zeta_2 + 301x - 32x\zeta_2 - 214x^2 + 96x^2\zeta_2 \right. \\
& \left. + Li_2(-x) (-32x^2) + Li_2(1-x) (4 - 8x) \right\} + \ln^2(x) \left\{ -\frac{19}{2} + 70x \right.
\end{aligned}$$



$$\begin{aligned}
& -38x^2 \Big\} + \ln^3(x) \Big\{ -3 + 6x - \frac{52}{3}x^2 \Big\} + \ln(1+x) \ln(x) \Big( -8 - 32x \\
& -24x^2 \Big) + \ln(1-x) \Big\{ 128 - 16\zeta_2 - 394x + 32x\zeta_2 + 272x^2 - 32x^2\zeta_2 \\
& + Li_2(1-x) \Big( -4 + 8x - 104x^2 \Big) + \ln(x) \Big( 56 - 256x + 216x^2 \Big) \\
& + \ln^2(x) \Big( 24 - 48x + 80x^2 \Big) \Big\} + \ln^2(1-x) \Big\{ -66 + 192x - 138x^2 \\
& + \ln(x) \Big( -42 + 84x - 132x^2 \Big) \Big\} + \ln^3(1-x) \Big\{ \frac{70}{3} - \frac{140}{3}x + \frac{140}{3}x^2 \Big\} \\
& + \ln \left( \frac{m_\phi^2}{\mu_F^2} \right) \Big\{ 54 - 8\zeta_2 - 172x + 16x\zeta_2 + 120x^2 - 16x^2\zeta_2 \\
& + Li_2(1-x) \Big( -48x^2 \Big) + \ln(x) \Big( 22 - 128x + 116x^2 \Big) + \ln^2(x) \Big( 8 - 16x \\
& + 32x^2 \Big) + \ln(1-x) \Big( -72 + 200x - 140x^2 \Big) + \ln(1-x) \ln(x) \Big( -40 \\
& + 80x - 128x^2 \Big) + \ln^2(1-x) \Big( 36 - 72x + 72x^2 \Big) \Big\} + \ln^2 \left( \frac{m_\phi^2}{\mu_F^2} \right) \Big\{ -15 \\
& + 36x - 24x^2 + \ln(x) \Big( -6 + 12x - 24x^2 \Big) + \ln(1-x) \\
& \times \Big( 12 - 24x + 24x^2 \Big) \Big\} \Big] \tag{51}
\end{aligned}$$

We now present the contributions resulting from pure  $t$ -channel processes where the final state quarks (anti-quarks) are non-identical (C and D in fig.(9)). The individual  $t$ -channel results are found to be identical and are given by

$$\begin{aligned}
\Delta_{q\bar{q}}^{(2),C\bar{C}} &= \Delta_{q\bar{q}}^{(2),D\bar{D}} = \Delta_{q\bar{q}}^{(2),C\bar{C}} = \Delta_{q\bar{q}}^{(2),D\bar{D}} = \Delta_{q\bar{q}}^{(2),C\bar{C}} = \Delta_{q\bar{q}}^{(2),D\bar{D}} \\
&= C_F T_f \left[ \frac{305}{9} - \frac{208}{27x} - \frac{32}{3x}\zeta_2 - 8\zeta_2 - \frac{470}{9}x + 8x\zeta_2 + \frac{703}{27}x^2 + \frac{32}{3}x^2\zeta_2 \right. \\
&+ S_{1,2}(1-x) \Big( 16 + 16x \Big) + Li_3(1-x) \Big( -32 - 32x \Big) + Li_2(1-x) \\
&\times \left( -4 + \frac{64}{3x} + 28x + \frac{32}{3}x^2 \right) + \ln(x) \left\{ \frac{62}{3} - 16\zeta_2 - \frac{176}{3}x - 16x\zeta_2 \right. \\
&\left. + \frac{40}{9}x^2 + Li_2(1-x) \Big( -8 - 8x \Big) \right\} + \ln^2(x) \left\{ -1 - 5x - \frac{40}{3}x^2 \right\}
\end{aligned}$$

$$\begin{aligned}
& + \ln^3(x) \left\{ \frac{10}{3} + \frac{10}{3}x \right\} + \ln(1-x) \left\{ -\frac{152}{3} + \frac{32}{9x} + \frac{200}{3}x - \frac{176}{9}x^2 \right. \\
& + Li_2(1-x)(32+32x) + \ln(x)(-8+32x+32x^2) \\
& + \ln^2(x)(-16-16x) \left. \right\} + \ln^2(1-x) \left\{ 8 + \frac{32}{3x} - 8x - \frac{32}{3}x^2 \right. \\
& + \ln(x)(16+16x) \left. \right\} + \ln\left(\frac{m_\phi^2}{\mu_F^2}\right) \left\{ -\frac{76}{3} + \frac{16}{9x} + \frac{100}{3}x - \frac{88}{9}x^2 \right. \\
& + Li_2(1-x)(16+16x) + \ln(x)(-4+16x+16x^2) \\
& + \ln^2(x)(-8-8x) + \ln(1-x) \left( 8 + \frac{32}{3x} - 8x - \frac{32}{3}x^2 \right) \\
& + \ln(1-x)\ln(x)(16+16x) \left. \right\} + \ln^2\left(\frac{m_\phi^2}{\mu_F^2}\right) \left\{ 2 + \frac{8}{3x} - 2x - \frac{8}{3}x^2 \right. \\
& \left. + \ln(x)(4+4x) \right\} \left. \right\} \quad (52)
\end{aligned}$$

If the final state quarks (anti-quarks) are identical, we find in addition to above mentioned  $t$ -channel processes, we have to include similar  $t$  processes with final state quarks (anti-quarks) interchanged (fig.(10)). Hence we have contributions from the additional  $t$  processes (fig.(10)) and their interferences with the already existing  $t$ -channel processes (fig.(9)). The former gives results identical to  $\Delta^{(2),C\bar{C}}$ ,  $\Delta^{(2),D\bar{D}}$  and  $\Delta^{(2),C\bar{D}}$ . The interference contributions are found to be

$$\begin{aligned}
\Delta_{qq}^{(2),C\bar{E}} &= \Delta_{qq}^{(2),D\bar{F}} = \Delta_{\bar{q}\bar{q}}^{(2),C\bar{E}} = \Delta_{\bar{q}\bar{q}}^{(2),D\bar{F}} \\
&= \left( C_F - \frac{C_A}{2} \right) C_F \left[ -34 - \frac{8}{1+x}\zeta_3 + 4\zeta_3 + 4\zeta_2 + 34x - 4x\zeta_3 \right. \\
&+ Li_3\left(\frac{1-x}{1+x}\right) \left( -32 + \frac{64}{1+x} + 32x \right) + Li_3\left(-\frac{1-x}{1+x}\right) \left( 32 \right. \\
&- \frac{64}{1+x} - 32x \left. \right) + S_{1,2}(-x) \left( 40 - \frac{32}{1+x} - 40x \right) + S_{1,2}(1-x) \\
&\times \left( -32 + \frac{64}{1+x} + 32x \right) + Li_3(-x) \left( 12 - \frac{16}{1+x} - 12x \right) \\
&+ Li_3(1-x) \left( 32 - \frac{64}{1+x} - 32x \right) + Li_2(-x)(8) + Li_2(1-x)
\end{aligned}$$

$$\begin{aligned}
& \times (24 + 8x) + \ln(x) \left\{ -18 + \frac{24}{1+x} \zeta_2 - 16\zeta_2 + 14x + 16x\zeta_2 \right. \\
& \left. + Li_2(-x) \left( -44 + \frac{64}{1+x} + 44x \right) + Li_2(1-x) \left( -24 + \frac{48}{1+x} + 24x \right) \right\} \\
& + \ln^2(x) \left\{ -4 - 10x \right\} + \ln^3(x) \left\{ \frac{10}{3} - \frac{16}{31+x} - \frac{10}{3}x \right\} + \ln(1+x) \\
& \times \left\{ -\frac{16}{1+x} \zeta_2 + 20\zeta_2 - 20x\zeta_2 + Li_2(-x) \left( 40 - \frac{32}{1+x} - 40x \right) \right. \\
& \left. + \ln(x) (8) + \ln^2(x) \left( -38 + \frac{56}{1+x} + 38x \right) \right\} + \ln^2(1+x) \ln(x) \\
& \times \left\{ 20 - \frac{16}{1+x} - 20x \right\} + \ln(1-x) \left\{ 32 - \frac{32}{1+x} \zeta_2 + 16\zeta_2 - 32x \right. \\
& \left. - 16x\zeta_2 + Li_2(-x) \left( 32 - \frac{64}{1+x} - 32x \right) + \ln(x) (16 + 16x) \right. \\
& \left. + \ln^2(x) \left( -8 + \frac{16}{1+x} + 8x \right) + \ln(1+x) \ln(x) \left( 32 - \frac{64}{1+x} - 32x \right) \right\} \\
& + \ln \left( \frac{m_\phi^2}{\mu_F^2} \right) \left\{ 16 - \frac{16}{1+x} \zeta_2 + 8\zeta_2 - 16x - 8x\zeta_2 + Li_2(-x) \left( 16 \right. \right. \\
& \left. \left. - \frac{32}{1+x} - 16x \right) + \ln(x) (8 + 8x) + \ln^2(x) \left( -4 + \frac{8}{1+x} + 4x \right) \right. \\
& \left. + \ln(1+x) \ln(x) \left( 16 - \frac{32}{1+x} - 16x \right) \right\} \Big] \tag{53}
\end{aligned}$$

and

$$\begin{aligned}
\Delta_{qq}^{(2),C\bar{F}} &= \Delta_{qq}^{(2),D\bar{E}} = \Delta_{q\bar{q}}^{(2),C\bar{F}} = \Delta_{q\bar{q}}^{(2),D\bar{E}} \\
&= \left( C_F - \frac{C_A}{2} \right) C_F \left[ -23 + 36x - 13x^2 + S_{1,2}(1-x) (4 - 8x - 8x^2) \right. \\
& \quad \left. + Li_3(1-x) (4 - 8x + 8x^2) + Li_2(1-x) (4 + 12x - 12x^2) \right. \\
& \quad \left. + \ln(x) \left\{ 2 - 4x + Li_2(1-x) (-8x^2) \right\} + \ln^2(x) (2 + 6x - 6x^2) \right] \tag{54}
\end{aligned}$$

$$+ \ln^3(x) \left( -\frac{4}{3}x^2 \right) \Big] \quad (55)$$

Finally we compute gluon gluon initiated processes that contribute to order  $a_s^2$ . Writing  $\Delta_{gg}^{(2)} = \Delta_{gg}^{(2),CA} + \Delta_{gg}^{(2),CF}$ , we find

$$\begin{aligned} \Delta_{gg}^{(2),CA} = & \frac{N^2}{N^2-1} \left[ -\frac{1}{3} + 8\zeta_3 - \frac{248}{3}x + 16x\zeta_3 - 4x\zeta_2 + 83x^2 + 16x^2\zeta_3 + \frac{8}{3}x^2\zeta_2 \right. \\ & + S_{1,2}(-x) (8 + 16x + 16x^2) + S_{1,2}(1-x) (-4 + 8x - 8x^2) \\ & + Li_3(-x) (12 + 24x + 24x^2) + Li_2(-x) \left( -8x + \frac{16}{3}x^2 \right) \\ & + \ln(x) \left\{ \frac{4}{3} - \frac{80}{3}x - 58x^2 + Li_2(-x) (-12 - 24x - 24x^2) \right\} \\ & + \ln^2(x) \left\{ 2x + \frac{50}{3}x^2 \right\} + \ln(1+x) \{ 4\zeta_2 + 8x\zeta_2 + 8x^2\zeta_2 \\ & + Li_2(-x) (8 + 16x + 16x^2) + \ln(x) \left( -8x + \frac{16}{3}x^2 \right) + \ln^2(x) \\ & \times \left( -6 - 12x - 12x^2 \right) \Big\} + \ln^2(1+x) \ln(x) \left\{ 4 + 8x + 8x^2 \right\} \Big] \quad (56) \end{aligned}$$

and

$$\begin{aligned} \Delta_{gg}^{(2),CF} = & S_{1,2}(-x) (-8 - 16x - 16x^2) + S_{1,2}(1-x) (-12 - 72x - 56x^2) \\ & + Li_3(-x) (-12 - 24x + 8x^2) + Li_3(1-x) (16 + 64x + 64x^2) \\ & + Li_2(-x) (8x) + Li_2(1-x) (-4 + 16x + 56x^2) + \ln(x) \\ & \times \left\{ -15 + 8\zeta_2 - 48x + 32x\zeta_2 + 121x^2 + 40x^2\zeta_2 + Li_2(-x) (12 \right. \\ & \left. + 24x + 8x^2) + Li_2(1-x) (-4 - 16x - 16x^2) \right\} + \ln^2(x) \left\{ -4 \right. \\ & \left. - 30x - 8x^2 \right\} + \ln^3(x) \left\{ -\frac{2}{3} - \frac{8}{3}x - \frac{16}{3}x^2 \right\} + \ln(1+x) \left\{ -4\zeta_2 \right. \\ & \left. - 8x\zeta_2 - 8x^2\zeta_2 + Li_2(-x) (-8 - 16x - 16x^2) + \ln(x) (8x) \right. \\ & \left. + \ln^2(x) (6 + 12x + 12x^2) \right\} + \ln^2(1+x) \ln(x) \left\{ -4 - 8x - 8x^2 \right\} \end{aligned}$$

$$\begin{aligned}
& + \ln(1-x) \left\{ 46 + 104x - 150x^2 + Li_2(1-x) \left( -16 - 64x - 64x^2 \right) \right. \\
& + \ln(x) \left( 20 + 64x - 16x^2 \right) + \ln^2(x) \left( 4 + 16x + 16x^2 \right) \left. \right\} \\
& + \ln^2(1-x) \left\{ -16 - 32x + 48x^2 + \ln(x) \left( -8 - 32x - 32x^2 \right) \right\} \\
& + \ln\left(\frac{m_\phi^2}{\mu_F^2}\right) \left\{ 23 + 52x - 75x^2 + Li_2(1-x) \left( -8 - 32x - 32x^2 \right) \right. \\
& + \ln(x) \left( 10 + 32x - 8x^2 \right) + \ln^2(x) \left( 2 + 8x + 8x^2 \right) + \ln(1-x) \\
& \times \left( -16 - 32x + 48x^2 \right) + \ln(1-x) \ln(x) \left( -8 - 32x - 32x^2 \right) \left. \right\} \\
& + \ln^2\left(\frac{m_\phi^2}{\mu_F^2}\right) \left\{ -4 - 8x + 12x^2 + \ln(x) \left( -2 - 8x - 8x^2 \right) \right\} \\
& -20 - 8\zeta_3 + 16\zeta_2 - 98x - 16x\zeta_3 + 36x\zeta_2 + 118x^2 + 8x^2\zeta_3 - 48x^2\zeta_2 \quad (57)
\end{aligned}$$

## References

- [1] H.P. Nilles, Phys.Rept. **110** (1989) 1;  
H.E. Haber and G.L. Kane, Phys.Rept. **117** (1985) 75;  
S. Dawson, Nucl.Phys. **B261** (1985) 297.
- [2] J.C. Pati and A. Salam, Phys.Rev. **D10** (1974) 275;  
H. Georgi and S.L. Glashow, Phys.Rev.Lett. **32** (1974) 438;  
For reviews, see P. Langacker, Phys.Rept. **72** (1981) 185.
- [3] P. Frampton, Phys.Rev. **D42** (1990) 3892;  
P. B. Pal and U. Sarkar, Phys.Rev. **D49** (1994) 3721.
- [4] L. E. Ibanez and G. G. Ross, Nucl. Phys. **B368** (1992) 3.
- [5] L. J. Hall and M. Suzuki, Nucl. Phys. **B231** (1984) 419.
- [6] A. Bouquet and P. Salati, Nucl.Phys. **B284** (1987) 557;  
A.E. Nelson and S.M. Barr, Phys.Lett. **B246** (1990) 141;  
E. Roulet and D. Tommasini, Phys.Lett. **B256** (1991) 218;  
B.A. Campbell, S. Davidson, J. Ellis and K. Olive, Phys.Lett. **B256** (1991) 457;  
W. Fischler, G. Giudice, R.G. Leigh and S. Paban, Phys.Lett. **B258** (1991) 45.
- [7] H. Dreiner and G.G. Ross, Nucl.Phys. **B410** (1993) 188.
- [8] S. Dimopoulos and L. J. Hall, Phys.Lett. **B207** (1988) 210;  
G. F. Giudice *et al.*, hep-ph/9602207;

- ECFA/DESY LC Physics Working Group, E. Accomando *et al.*, Phys.Rept. **299** (1998) 1;  
 J. Erler, J. L. Feng, and N. Polonsky, Phys.Rev.Lett. **78** (1997) 3063;  
 J. Kalinowski, R. Rückl, H. Spiesberger, and P. M. Zerwas, Phys.Lett. **B406** (1997) 314.
- [9] V. Barger, G. F. Giudice, and T. Han, Phys.Rev. **D40** (1989) 2987.
- [10] S. Dimopoulos *et al.*, Phys.Rev. **D41** (1990) 2099;  
 H. Dreiner and G. G. Ross, Nucl.Phys. **B365** (1991) 597;  
 B. C. Allanach *et al.*, hep-ph/9906224;  
 H. Dreiner, P. Richardson, and M. H. Seymour, JHEP **0004** (2000) 008.
- [11] A. Datta *et al.*, Phys.Rev. **D56** (1997) 3107;  
 J.-M. Yang *et al.*, hep-ph/9802305;  
 R. J. Oakes *et al.*, Phys.Rev. **D57** (1998) 534;  
 E. L. Berger, B. W. Harris, and Z. Sullivan, Phys.Rev.Lett. **83** (1999) 4472.
- [12] J.L. Hewett, Snowmass Summer Study (1990);  
 J. Butterworth and H. Dreiner, Nucl.Phys. **B397** (1993) 3;  
 D. Choudhury and S. Raychaudhuri, Phys.Lett. **B401** (1997) 54;  
 G. Altarelli *et al.*, Nucl.Phys. **B506** (1997) 3;  
 J. Kalinowski *et al.*, Z.Phys. **C74** (1997) 595;  
 T. Kon and T. Kobayashi, Phys.Lett. **B409** (1997) 265;  
 G. Altarelli, G.F. Giudice, and M.L. Mangano, Nucl.Phys. **B506** (1997) 29;  
 J. Ellis, S. Lola, and K. Sridhar, Phys.Lett. **B408** (1997) 252;  
 M. Carena *et al.*, Phys.Lett. **B414** (1997) 92.
- [13] J. Kalinowski *et al.*, Phys.Lett. **B414** (1997) 297;  
 J. L. Hewett and T. G. Rizzo, hep-ph/9809525;  
 H. Dreiner, P. Richardson, and M. H. Seymour, hep-ph/9903419; hep-ph/0001224;  
 G. Moreau, M. Chemtob, F. Deliot, C. Royon, and E. Perez, Phys.Lett. **B475** (2000) 184;  
 G. Moreau, E. Perez, and G. Polesello, hep-ph/0002130; Nucl.Phys. **B604** (2001) 3;  
 S. Abdullin *et al.*, hep-ph/0005142.
- [14] K. Agashe and M. Graesser, Phys.Rev. **D54** (1995) 4445;  
 D. Choudhury and P. Roy, Phys.Lett. **B378** (1996) 153;  
 F. Vissani and A.Yu. Smirnov, Phys.Lett. **B380** (1996) 317.
- [15] Debajyoti Choudhury, Swapan Majhi and V. Ravindran Nucl.Phys. **B660** (2003) 343; JHEP **0601** (2006) 027.
- [16] H.K. Dreiner, S. Grab, M. Kramer and M.K. Trenkel, Phys.Rev. **D75** (2007) 035003;  
 Li Lin Yang, Chong Sheng Li, Jian Jun Liu and Qiang Li, Phys.Rev. **D72** (2005) 074026.
- [17] CDF Collaboration (Darin E. Acosta *et al.*) Phys.Rev.Lett. **91** (2003) 171602;  
 Phys.Rev.Lett. **95** (2005) 131801;

- CDF Collaboration (A. Abulencia et al.) Phys.Rev.Lett. **95** (2005) 252001;  
 Phys.Rev.Lett. **96** (2006) 211802;  
 CDF Collaboration (T. Aaltonen et al.) Phys.Rev.Lett. **102** (2009) 091805.
- [18] D0 Collaboration (V.M. Abazov et al.) Phys.Rev.Lett. **97** (2006) 111801.
- [19] G. Bhattacharyya, Nucl.Phys. B (Proc. Suppl.) **52A** (1996) 83;  
 H. Dreiner, hep-ph/9707435 v2;  
 R. Barbier *et al.*, hep-ph/9810232;  
 B. C. Allanach, A. Dedes and H. K. Dreiner, Phys. Rev. D **60** (1999) 075014;  
 R. Barbier *et al.*, Phys. Rept. **420** (2005) 1;  
 M. Chemtob, Prog. Part. Nucl. Phys. **54** (2005) 71.
- [20] H. Klapdor-Kleingrothaus *et al.*, Prog.Part.Nucl.Phys. **32** (1994) 261;  
 M. Hirsch, H. V. Klapdor-Kleingrothaus, and S. G. Kovalenko, Phys.Rev.Lett. **75**  
 (1995) 17; Phys.Rev. **D53** (1996) 1329;  
 K. S. Babu and R. N. Mohapatra, Phys.Rev.Lett. **75** (1995) 2276;  
 J. W. F. Valle, hep-ph/9509306.
- [21] A.I. Belesev *et al.*, Phys.Lett. **B350** (1995) 263;  
 C. Weinheimer *et al.*, Phys.Lett. **B300** (1993) 210.
- [22] G. Bhattacharyya and D. Choudhury, Mod.Phys.Lett. **A10** (1995) 1699.
- [23] A. S. Joshipura, V. Ravindran and S. K. Vempati, Phys.Lett. **B451** (1999) 98.
- [24] S. Davidson, D. Bailey and B. Campbell Z.Phys. **C61** (1994) 613;  
 C.S. Wood, *Science* **279** (1997) 1759;  
 W.J. Marciano and J.L. Rosner, Phys.Rev.Lett. **65** (1990) 2963;  
 W.J. Marciano, 1997 INT Summer Workshop.
- [25] S.A. Larin, J.A.M. Vermaseren, Phys.Lett. **B303** (1993) 334;  
 T. van Ritbergen, J.A.M. Vermaseren, S.A. Larin, Phys.Lett. **B400** (1997) 379;  
 M. Czakon, Nucl.Phys. **B710** (2005) 485.
- [26] J.A.M. Vermaseren, S.A. Larin, T. van Ritbergen, Phys.Lett. **B405** (1997) 327.
- [27] T. Matsuura, thesis Leiden University, 1989;  
 S. Dawson, Nucl.Phys. **B359** (1991) 283;  
 A. Djouadi, M. Spira, P. Zerwas, Phys.Lett. **B264** (1991) 440.
- [28] G. Kramer and B. Lampe, Z.Phys. **C34** (1987) 497 [Erratum: **C42** (1989) 504];  
 T. Matsuura and W.L. van Neerven, Z.Phys. **C38** (1988) 623;  
 T. Matsuura S.C. van der Marck and W.L. van Neerven, Phys.Lett. **B211** (1988)  
 171; Nucl.Phys. **B319** (1989) 570;  
 W.L. van Neerven, Nucl.Phys. **B268** (1986) 453;  
 R.J. Gonsalves, Phys.Rev. **D28** (1983) 1542 ;  
 R.V. Harlander, Phys.Lett. **B492** (2000) 74.
- [29] G. Passarino and M. J. G. Veltman, Nucl.Phys. **B160** (1979) 151

- [30] R. E. Cutkosky, *J. Math. Phys.* **1** (1960) 429;  
W. L. van Neerven, *Nucl. Phys. B* **268** (1986) 453;  
V. Ravindran, J. Smith and W. L. van Neerven, *Nucl. Phys. B* **704** (2005) 332.
- [31] T. Matsuura and W.L. van Neerven, *Z.Phys.* **C38** (1988) 623;  
T. Matsuura S.C. van der Marck and W.L. van Neerven, *Phys.Lett.* **B211** (1988) 171; *Nucl.Phys.* **B319** (1989) 570;  
T. Matsuura, thesis Leiden University, 1989;  
R.K.Ellis, M.A.Furman, H.E. Haber and I. Hinchliff, *Nucl.Phys.* **B173** (1980) 397;  
J. Smith, D. Thomas and W.L. van Neerven, *Z.Phys.* **C44** (1989) 267;  
W. Beenakker, H. Kuijf, W.L. van Neerven, J. Smith, *Phys.Rev.* **D40** (1989) 54;  
V. Ravindran, J. Smith, W.L. van Neerven, *Pramana* **62** (2004) 683.
- [32] FORM by J.A.M. Vermaseren, version 3.0 available from <http://www.nikhef.nl/form>;  
arXiv:math-ph/0010025.
- [33] F. Block and A. Nordsieck, *Phys.Rev.* **52** (1937) 54;  
D.R. Yannie, S.C. Frautschi and H. Suura, *Ann.Phys.(N.Y.)* **13** (1961) 379.
- [34] T. Kinoshita, *J.Math.Phys.* **3** (1962) 650;  
T.D. Lee and M. Nauenberg, *Phys.Rev.* **133** (1964) B1549;  
N. Nakanishi, *Prog.Theor.Phys.* **19** (1958) 159
- [35] R. Hamberg, W. L. van Neerven and T. Matsuura, *Nucl. Phys. B* **359** (1991) 343;  
R. V. Harlander and W. B. Kilgore, *Phys. Rev. Lett.* **88** (2002) 201801;  
C. Anastasiou and K. Melnikov, *Nucl. Phys. B* **646** (2002) 220;  
V. Ravindran, J. Smith and W. L. van Neerven, *Nucl. Phys. B* **665** (2003) 325.
- [36] G. Altareli and G. Parisi, *Nucl.Phys.* **B126** (1977) 298;  
G. Curci W. Furmanski and R. Petronzio, *Nucl.Phys.* **B175** (1980) 27;  
W. Furmanski and R. Petronzio, *Phys.Lett.* **B97** (1980) 437;  
E.G. Floratos, D.A. Ross and C.T. Sachrajda, *Nucl.Phys.* **B129** 66 (1977); erratum:  
*ibid* **B139** (1978) 545; *ibid.* **B152** (1979) 493.
- [37] Robert V. Harlander and William B. Kilgore *Phys.Rev.* **D68** (2003) 013001.
- [38] S. Moch, J. A. M. Vermaseren and A. Vogt, *Nucl.Phys.* **B688** (2004) 101.
- [39] A. Vogt, S. Moch and J. A. M. Vermaseren, *Nucl.Phys.* **B691** (2004) 129.
- [40] S. Moch, J. A. M. Vermaseren and A. Vogt, *JHEP* **0508** (2005) 049.
- [41] S. Moch, J. A. M. Vermaseren and A. Vogt, *Phys.Lett.* **B625** (2005) 245.
- [42] S. Moch, J. A. M. Vermaseren and A. Vogt, *Nucl.Phys.* **B726** (2005) 317
- [43] J. Blumlein and J. A. M. Vermaseren, *Phys.Lett.* **B606** (2005) 130.
- [44] S. Moch and A. Vogt, *Phys.Lett.* **B631** (2005) 48.
- [45] E. Laenen and L. Magnea, *Phys.Lett.* **B632** (2006) 270.



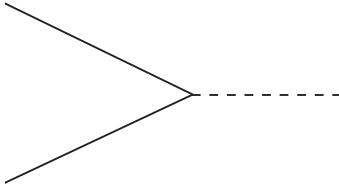


Figure 1: Subprocess  $q_i + \bar{q}_j \rightarrow \phi$ .

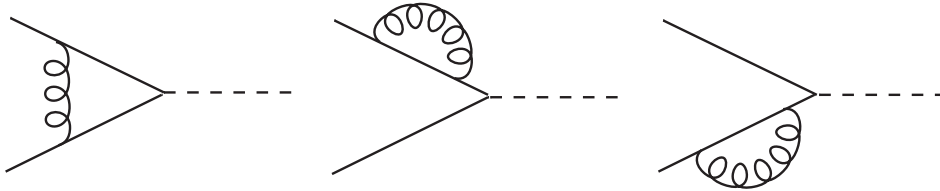


Figure 2: Subprocess  $q_i + \bar{q}_j \rightarrow \phi$ .

- [46] A. Idilbi, X. d. Ji, J. P. Ma and F. Yuan, Phys.Rev. **D73** (2006) 077501.
- [47] V. Ravindran, Nucl.Phys. **B746** (2006) 58.
- [48] J. Blumlein, V. Ravindran and W. L. van Neerven, Nucl.Phys. **B586** (2000) 349.
- [49] J. Blumlein and V. Ravindran, Nucl.Phys. **B716** (2005) 128
- [50] Y. L. Dokshitzer, G. Marchesini and G. P. Salam, Phys.Lett. **B634** (2006) 504.
- [51] V. Ravindran, Nucl.Phys. **B752** (2006) 173
- [52] A.D. Martin, W.J. Stirling, R.S. Thorne and G. Watt Eur.Phys.J. **C63** (2009) 189,  
Eur.Phys.J. **C64** (2009) 653.
- [53] T. Plehn, Phys.Rev. **D67** (2003) 014018;  
F. Maltoni, Z. Sullivan and S. Willenbrock, Phys.Rev. **D67** (2003) 093005.

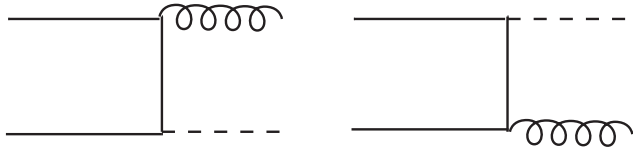


Figure 3: Subprocess  $q_i + \bar{q}_j \rightarrow \phi + g$ .

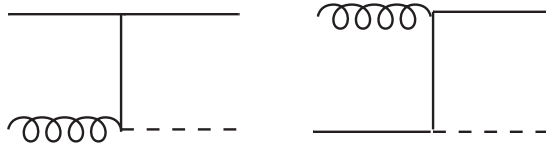


Figure 4: Subprocess  $q_i + g \rightarrow \phi + q_j$ .

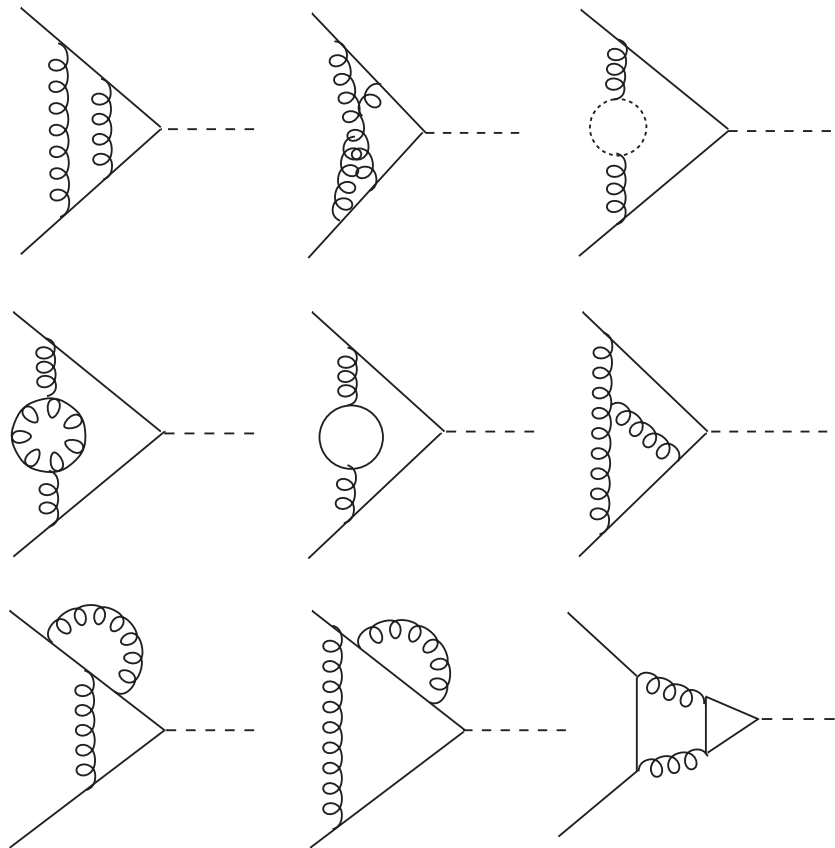


Figure 5: Subprocess  $q_i + \bar{q}_j \rightarrow \phi$ .

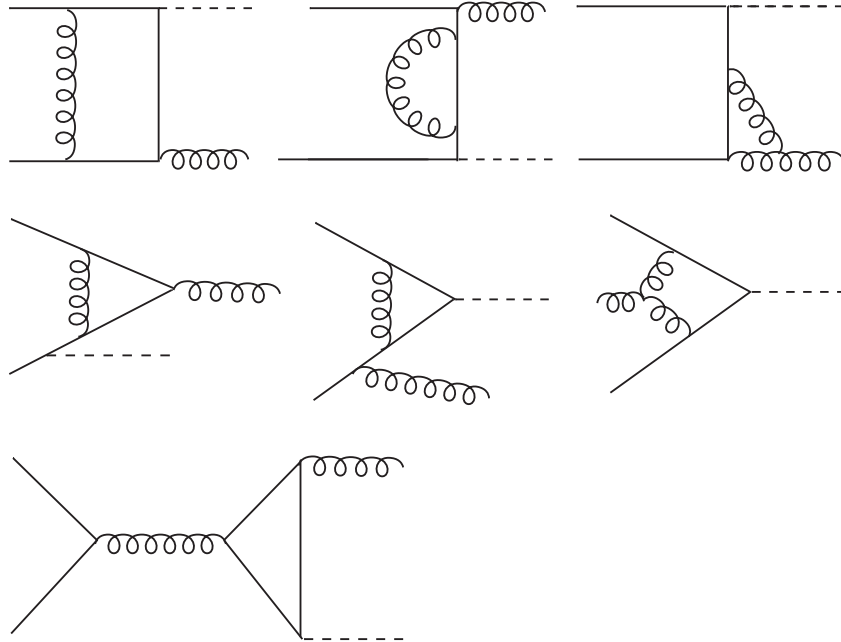


Figure 6: Subprocess  $q_i + \bar{q}_j \rightarrow \phi + g$ .

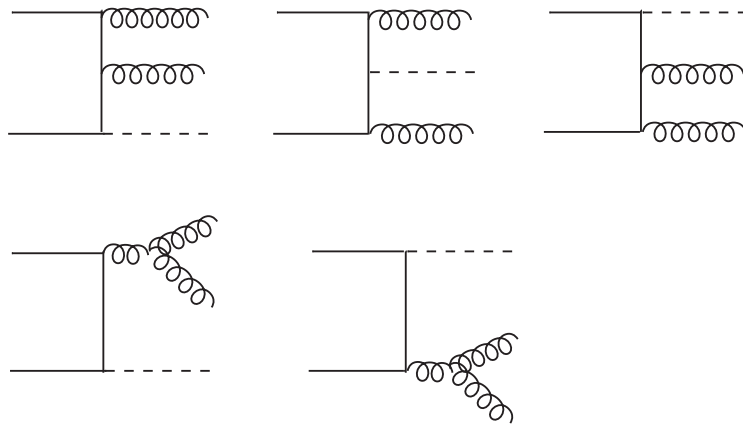


Figure 7: Subprocess  $q_i + \bar{q}_j \rightarrow \phi + g + g$ .

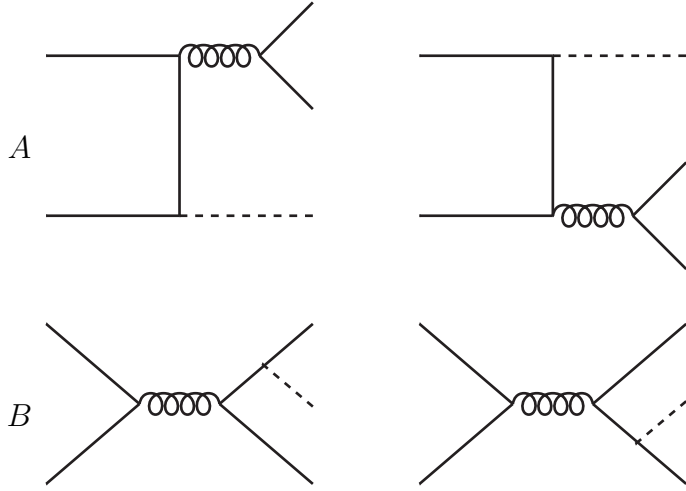


Figure 8:  $s$  channel annihilation graphs contributing to the subprocess  $q_i + \bar{q}_j \rightarrow \phi + q_k + \bar{q}_l$ .

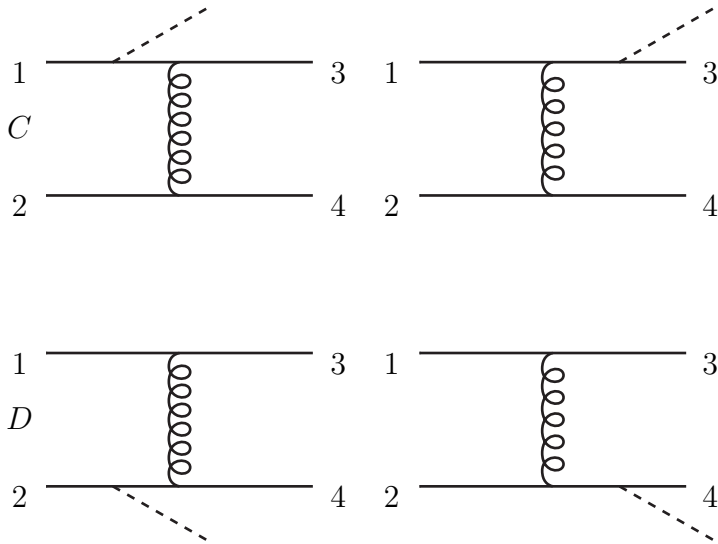


Figure 9:  $t$  channel gluon exchange graphs contributing to the subprocesses  $q_i + \bar{q}_j \rightarrow \phi + q_k + \bar{q}_l$ ,  $q_i + q_j \rightarrow \phi + q_k + q_l$  and  $\bar{q}_i + \bar{q}_j \rightarrow \phi + \bar{q}_k + \bar{q}_l$ .

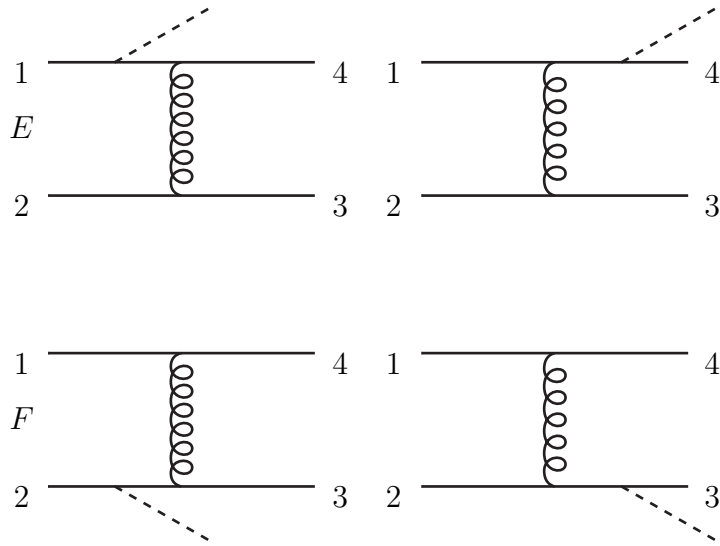


Figure 10:  $t$  channel gluon exchange graphs contributing to the subprocesses  $q(\bar{q}) + q(\bar{q}) \rightarrow \phi + q(\bar{q}) + q(\bar{q})$  with identical quarks (anti-quarks).

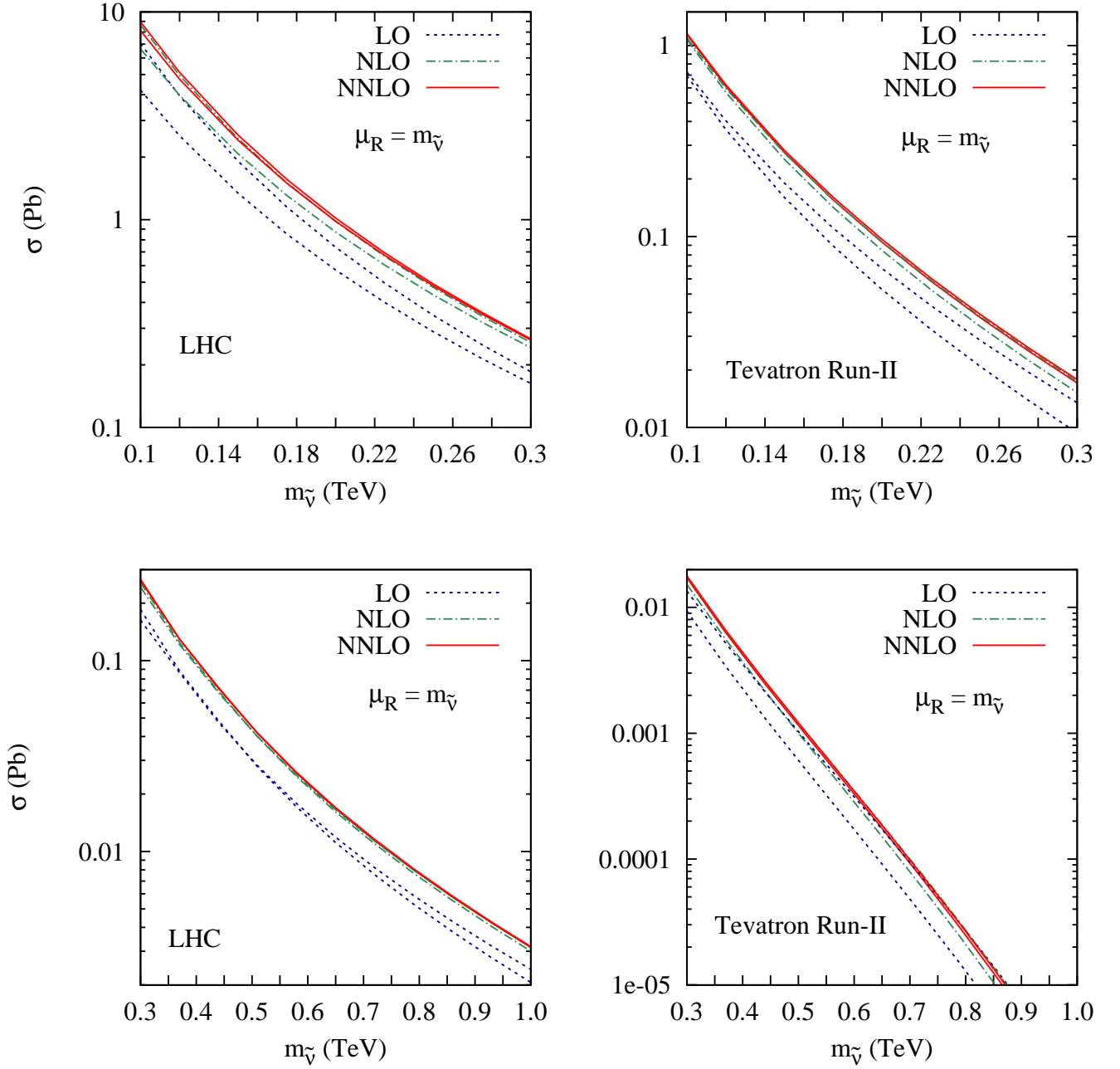


Figure 11: Total cross-section for the  $\tilde{\nu}$  production. The upper (lower) set of lines correspond to the factorisation scale  $\mu_F = m_{\tilde{\nu}}$  ( $0.1 m_{\tilde{\nu}}$ ).

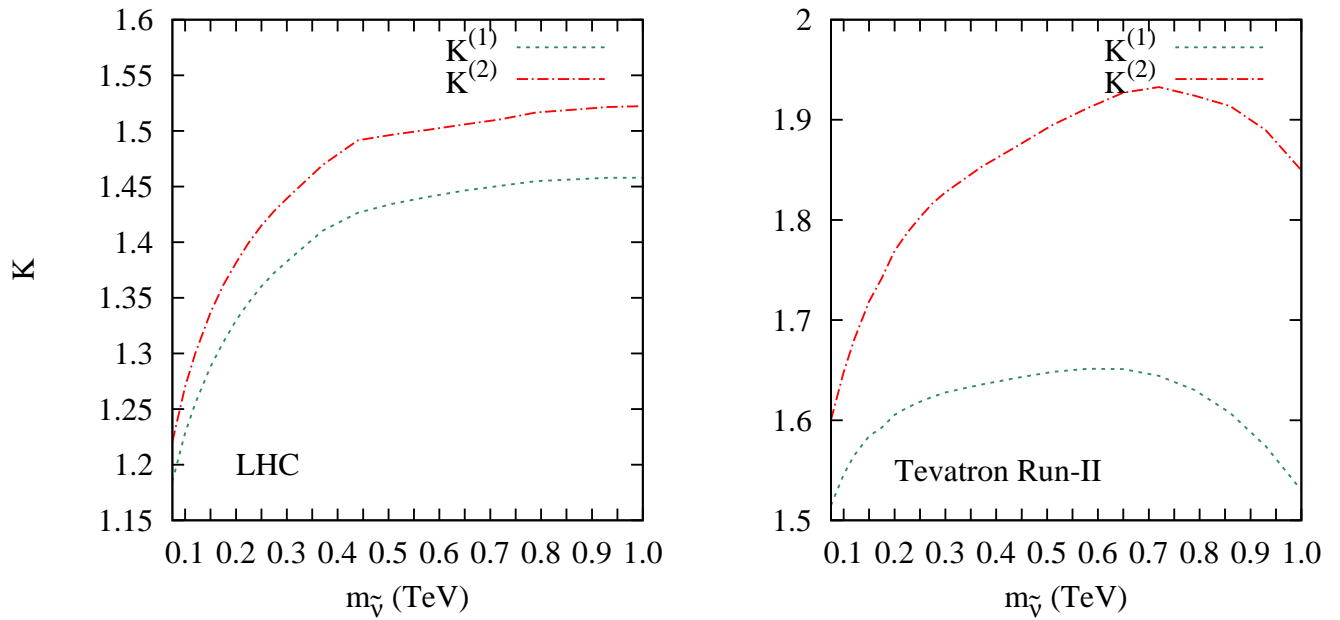


Figure 12:  $K$ -factor for the  $\tilde{\nu}$  production.



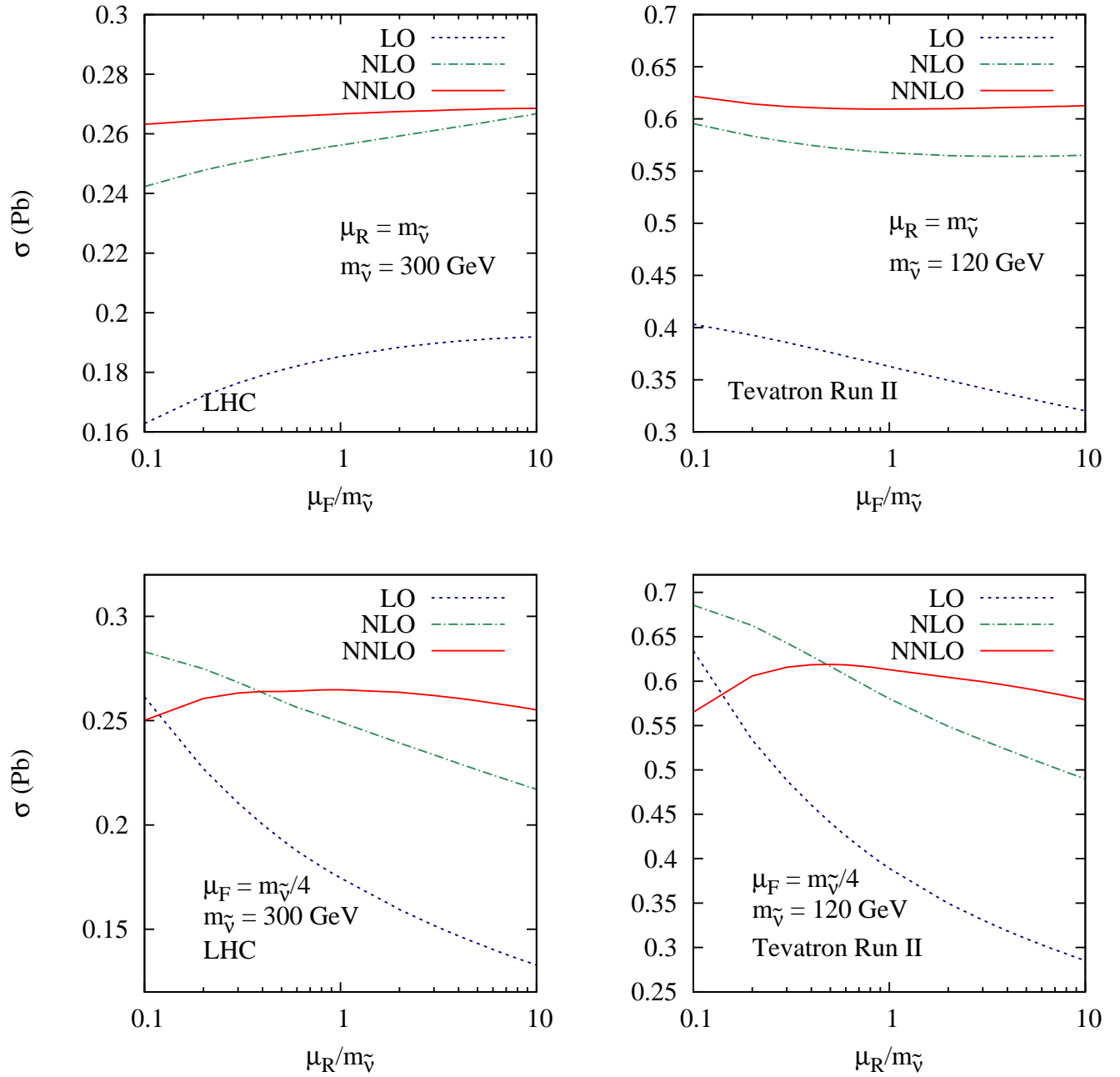


Figure 13:  $\mu_F$  and  $\mu_R$  variations for the  $\tilde{\nu}$  production.

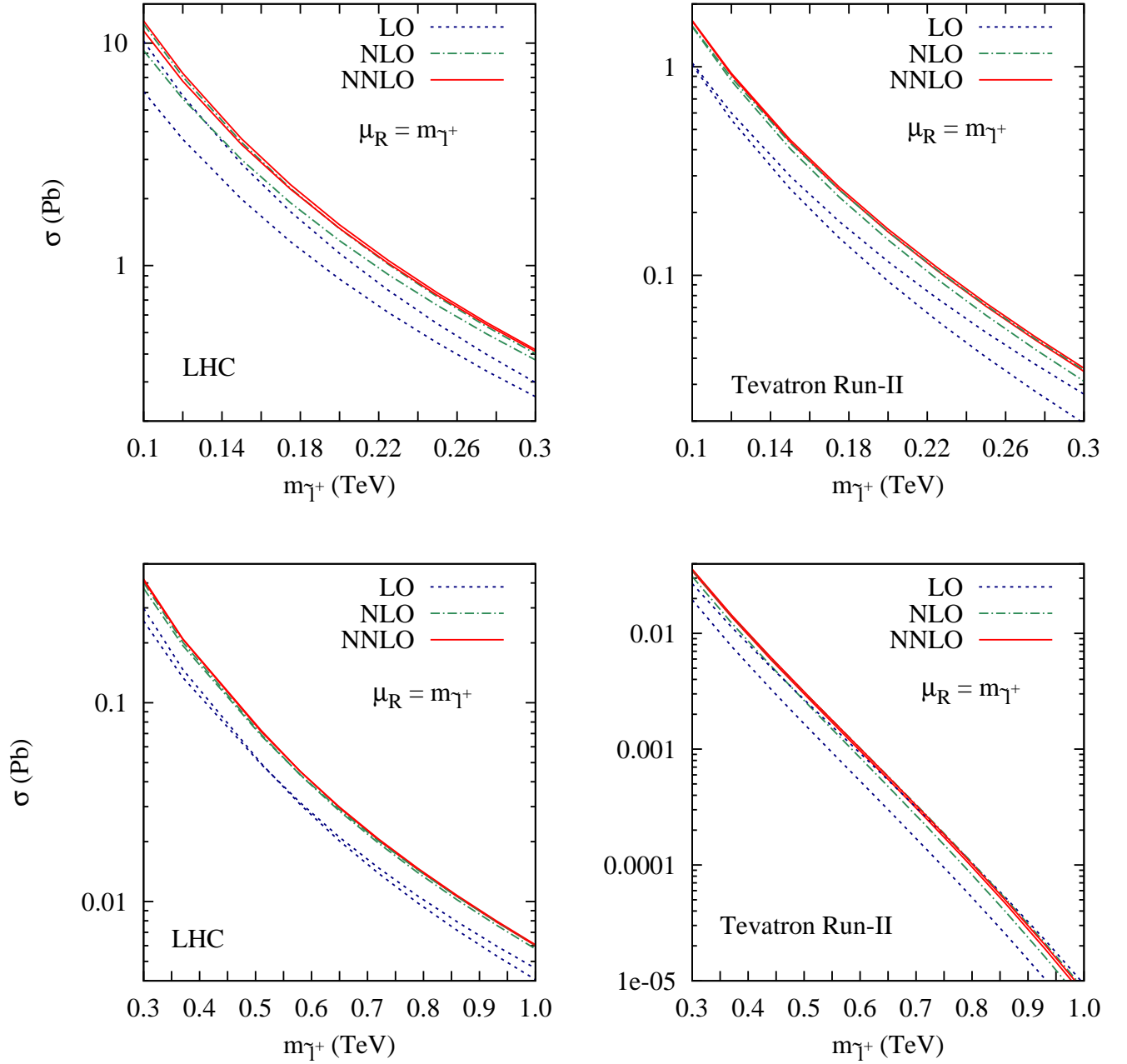


Figure 14: Total cross-section for the  $\tilde{\ell}^+$  production. The upper (lower) set of lines correspond to the factorisation scale  $\mu_F = m_{\tilde{\ell}^+}$  ( $0.1m_{\tilde{\nu}}$ ).

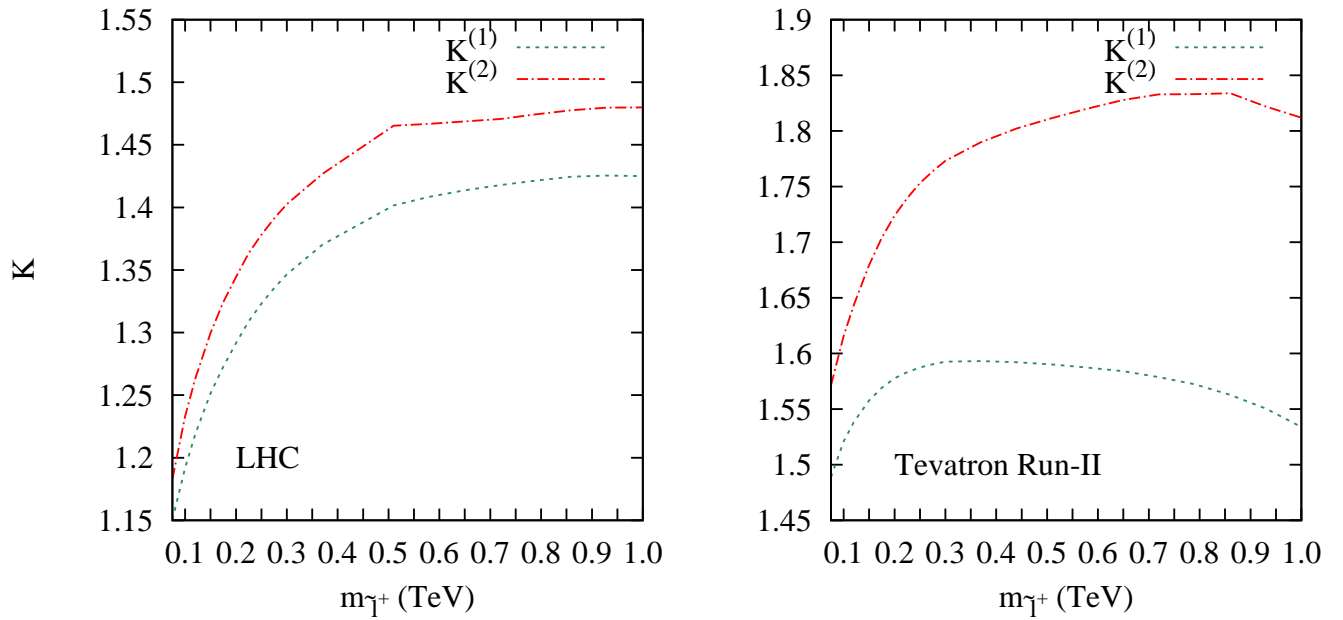


Figure 15:  $K$ -factor for the  $\tilde{\ell}^+$  production.

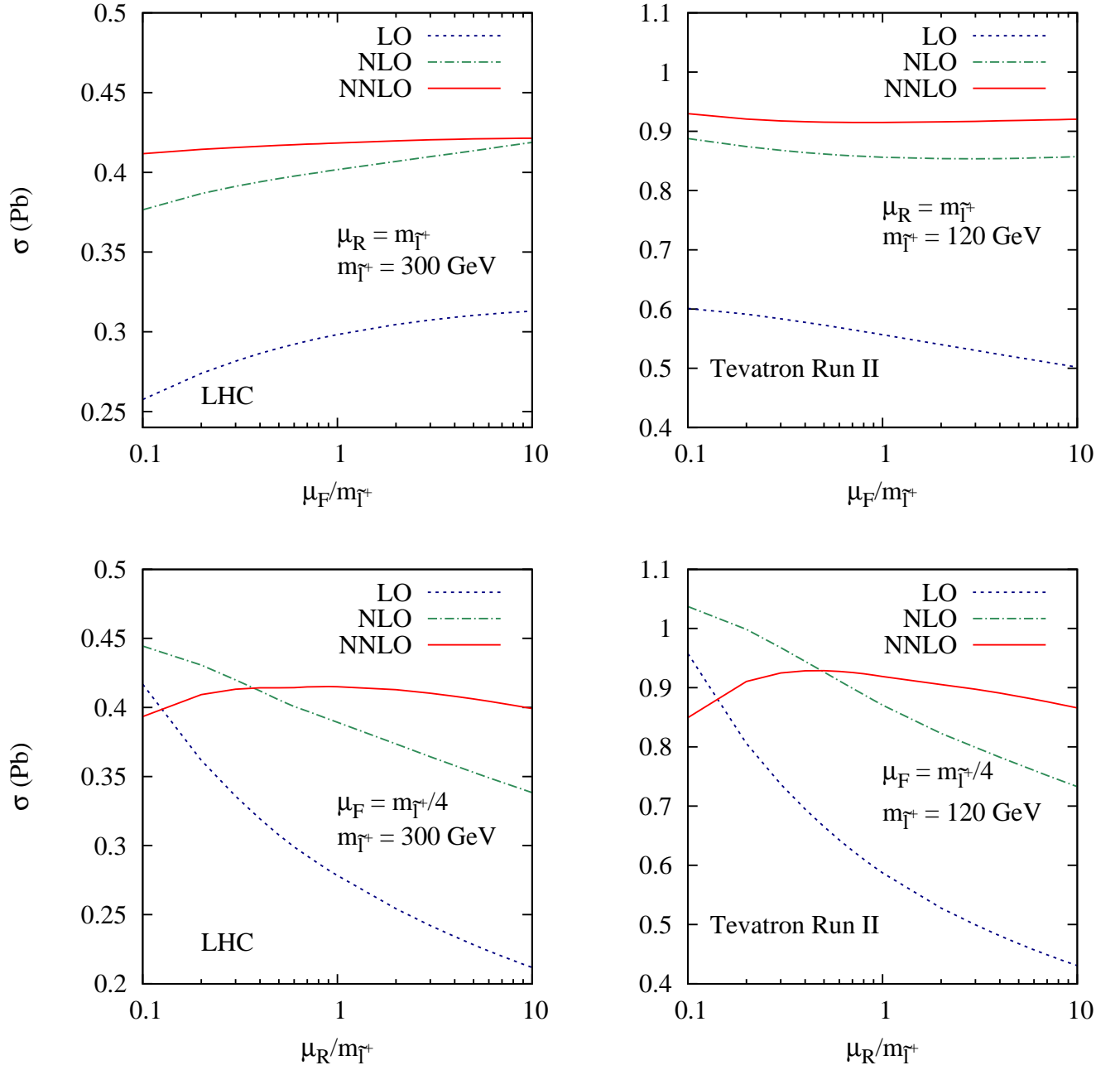


Figure 16:  $\mu_F$  and  $\mu_R$  variations for the  $\tilde{\ell}^+$  production.

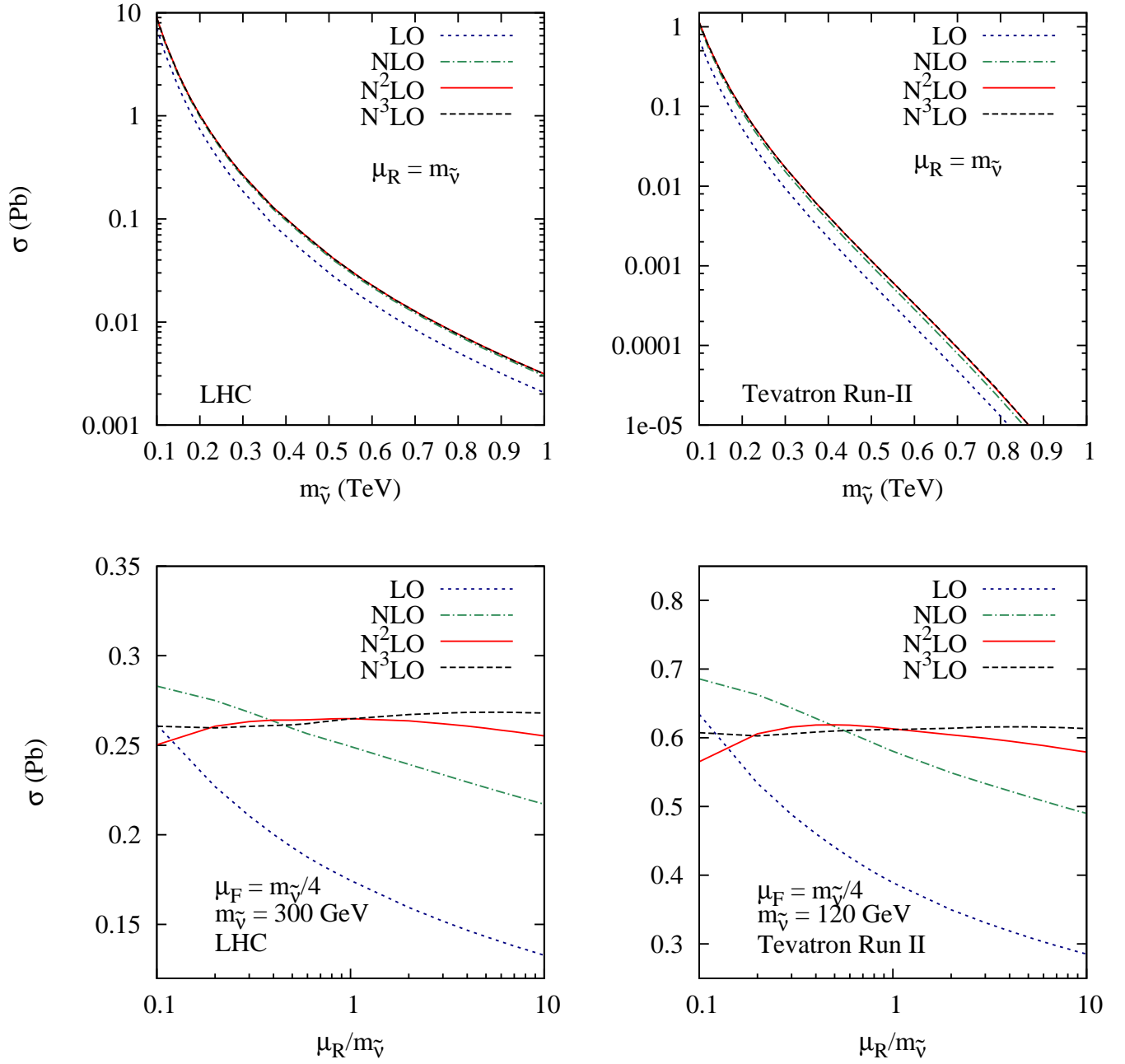


Figure 17: Total cross section and  $\mu_R$  variations for the  $\tilde{\nu}$  production.